

---

---

# Atomistic Modelling of Aggregate Chlorophyll Systems

---

---

By

OLIVER J. H. FEIGHAN



School of Chemistry  
UNIVERSITY OF BRISTOL

A dissertation submitted to the University of Bristol in accordance with the requirements of the degree of DOCTOR OF PHILOSOPHY in the Faculty of Science.

JANUARY, 2022

Word count: 0



## **ABSTRACT**

**H**ere goes the abstract



## **DEDICATION AND ACKNOWLEDGEMENTS**

**H**ere goes the dedication.



## AUTHOR'S DECLARATION

I declare that the work in this dissertation was carried out in accordance with the requirements of the University's Regulations and Code of Practice for Research Degree Programmes and that it has not been submitted for any other academic award. Except where indicated by specific reference in the text, the work is the candidate's own work. Work done in collaboration with, or with the assistance of, others, is indicated as such. Any views expressed in the dissertation are those of the author.

SIGNED: ..... DATE: .....



## TABLE OF CONTENTS

	<b>Page</b>
<b>List of Tables</b>	<b>xi</b>
<b>List of Figures</b>	<b>xiii</b>
<b>1 Introduction</b>	<b>1</b>
1.1 Quantum Exploits in Light Harvesting Systems . . . . .	1
1.1.1 Electronic Energy Transfer . . . . .	1
1.1.2 Coherence . . . . .	1
1.2 Light-Matter Response . . . . .	1
1.3 Electronic Structure for Large Systems . . . . .	1
1.4 The Aim . . . . .	1
<b>2 Mean-Field excited states</b>	<b>3</b>
2.1 Theory . . . . .	3
2.1.1 $\Delta$ -SCF and eigenvalue difference . . . . .	3
2.1.2 Eigenvalue Difference . . . . .	5
2.1.3 Transition Density and Dipole Moments . . . . .	5
2.1.4 Semi-empirical extensions . . . . .	6
2.2 Benchmarking . . . . .	8
2.2.1 Reference Data and test set . . . . .	8
2.2.2 Small Systems . . . . .	9
2.2.3 Non-orthogonality . . . . .	12
2.2.4 LHII Chlorophyll . . . . .	14
2.2.5 xTB methods . . . . .	17
2.3 Conclusions and Further Work . . . . .	22
2.3.1 Embedding . . . . .	23
2.3.2 Scaling . . . . .	23
<b>3 Chlorophyll specific methods</b>	<b>27</b>
3.1 The Cassida equation . . . . .	27

---

**TABLE OF CONTENTS**

---

3.1.1	Approximations to Solutions . . . . .	27
3.1.2	MNOK Integrals . . . . .	27
3.2	Parameterization . . . . .	27
3.2.1	Reference Data . . . . .	27
3.2.2	Objective Function . . . . .	27
3.2.3	Minimization Algorithms . . . . .	27
3.3	Benchmarking . . . . .	27
3.3.1	Transition properties . . . . .	27
3.3.2	Potential Energy Surfaces . . . . .	27
3.3.3	Absorption Spectra . . . . .	27
<b>4</b>	<b>Exciton Method</b>	<b>45</b>
4.1	Theory . . . . .	45
4.1.1	Exciton States . . . . .	45
4.1.2	Embedding . . . . .	45
4.2	Truncated Chlorophylls . . . . .	45
4.2.1	Rotation . . . . .	45
4.2.2	Distance . . . . .	45
4.3	LHII Pairs . . . . .	45
4.3.1	Assignment of States . . . . .	45
4.3.2	Comparison . . . . .	45
<b>5</b>	<b>Atomistic Modelling of Light Harvesting Complexes</b>	<b>51</b>
5.1	LHII . . . . .	59
5.1.1	Spectral Density Method . . . . .	59
5.1.2	Molecular Dynamics Method . . . . .	59
5.2	Approximating Spectral Densities . . . . .	59
5.2.1	Hessians . . . . .	59
5.2.2	Huang Rhys Factors . . . . .	59
5.2.3	Chlorophyll distances . . . . .	59
5.3	Environmental Effects . . . . .	59
5.3.1	Screening . . . . .	59
5.3.2	Embedding . . . . .	59
5.4	Sites, states and couplings . . . . .	59
5.4.1	Sites . . . . .	59
5.4.2	Exciton states . . . . .	59
5.4.3	Coupling . . . . .	59
5.5	Excitation Energies . . . . .	59

---

TABLE OF CONTENTS

<b>6 Discussion</b>	<b>61</b>
6.1 Transition Property Approximations . . . . .	61
6.2 Further Investigations into LHII . . . . .	61
6.3 Coherence . . . . .	61
<b>A Appendix A</b>	<b>63</b>
A.1 Electronic Structure Codes . . . . .	63
A.2 Computational Hardware . . . . .	63
<b>Bibliography</b>	<b>65</b>



## LIST OF TABLES

TABLE	Page
-------	------



## LIST OF FIGURES

<b>FIGURE</b>	<b>Page</b>
2.1 Transition energies $\Delta E$ from TD-DFT (black) and $\Delta$ -SCF (red) plotted against EOM-CCSD energies, with the line $y = x$ (dashed) for reference. The ethene dimer outlier has been circled. . . . .	10
2.2 Transition dipole magnitudes from TD-DFT (black) and $\Delta$ -SCF (red) plotted against EOM-CCSD transition dipole magnitudes, with the line $y = x$ (dashed) for reference. . . . .	11
2.3 The absolute value of the error in transition dipole magnitude between $\Delta$ -SCF and EOM-CCSD, plotted against the $\Delta$ -SCF overlap of the ground and excited state. All systems were translated by 100 Å in all cartesian axes. Transition dipole magnitudes calculated without any correction are shown in red, whilst those with the symmetric orthogonalisation correction are shown in black. . . . .	13
2.4 The transition energies from $\Delta$ -SCF for the 26 chlorophyll geometries, plotted against energies from TD-DFT. The line of best fit ( $R^2 = 0.87$ ) is shown as the dashed line. . . . .	15
2.5 The transition dipole magnitudes from $\Delta$ -SCF for the 26 chlorophyll geometries, plotted against dipole magnitudes from TD-DFT. The line of best fit ( $R^2 = 0.57$ ) is shown as the dashed line. . . . .	16
2.6 The errors of several levels of theory at predicting CC2 transition energies. . . . .	18
2.7 A breakdown of the symmetry orbitals in STO-3G methane into the subspaces present in the $T_d$ point group. . . . .	20
3.1 correlations of energies . . . . .	28
3.2 correlations of transition dipole moments . . . . .	29
3.3 Nelder-mead . . . . .	30
3.4 SLSQP . . . . .	31
3.5 optimized parameters from SLSQP procedure. . . . .	31
3.6 training scatter . . . . .	32
4.1 caption . . . . .	46
4.2 caption . . . . .	47



## INTRODUCTION

Naturally occurring light harvesting systems present an interesting scientific challenge. With near perfect efficiency, the energy from a photon will be taken and transferred to a reaction centre, leading to charge transfer processes that culminate in powering biological systems. Making models that can predict and explain these effects are key to making similarly efficient photovoltaic systems.

### 1.1 Quantum Exploits in Light Harvesting Systems

Begins a section.

#### 1.1.1 Electronic Energy Transfer

Begins a subsection.

#### 1.1.2 Coherence

### 1.2 Light-Matter Response

### 1.3 Electronic Structure for Large Systems

### 1.4 The Aim



## MEAN-FIELD EXCITED STATES

This chapter collates all of the work done on investigating and benchmarking  $\Delta$ -SCF methods, at both an ab initio DFT level of theory as well as with semi-empirical, tight-binding approximations. The reduced cost and moderate accuracy of these methods make them an ideal substitute for full TD-DFT or high-level methods when investigating large systems like chlorophyll. Transition properties were calculated for a range of molecules, as well as for a small set of chlorophyll geometries, using variety of different basis sets, density functionals, response methods and electronic structure methods. Most of the work was compared to a high-standard EOM-CCSD reference, from which conclusion were made on the accuracy of each method. The Non-orthogonality issue of the ground and excited states were also for the mean-field  $\Delta$ -SCF method, as well as assignment of transitions based on symmetry. These investigations, as well as the work on using semi-empirical methods, is all novel work. It was found that while the high-level methods give reasonable results, the semi-empirical  $\Delta$ -SCF methods are not as accurate. This results is unexpected in the context of the benchmarking, however has reasonable explanations, and will guide the work of the later chapter on developing a new semi-empirical method. This work sets the groundwork of what could be reasonably achieved against the goals set out in the introduction chapter.

### 2.1 Theory

#### 2.1.1 $\Delta$ -SCF and eigenvalue difference

$\Delta$ -SCF predicts the transition energy  $\Delta E$  of a system as the difference of the single point energy  $E_n$  of two states:

$$(2.1) \quad \Delta E = E_2 - E_1$$

Finding the excited state correctly can be an issue, as for ease is usually assumed to be similar to the ground state. In its simplest form, the  $\Delta$ -SCF method calculates the ground state with normal DFT or other mean-field methods, and then calculates the excited state by rerunning the same method with the excited state occupation numbers. A full description of both the ground as excited state is given as the orbital coefficients output from the two calculations.

Initially, the excited state was calculated by relaxing the orbitals which contain the excited electron and hole in the ground state space, so that the excited state and ground state are orthogonal[8]. However, it was argued that this procedure would exacerbate errors from finding the ground state, and that the excited state was not a proper SCF solution[3]. Alternatively, an SCF like method was proposed, where instead of populating orbitals according to the aufbau principle, orbitals which most resemble the previous iteration's orbitals should be occupied. Each iteration in an SCF procedure produces new molecular orbital coefficients by solving the Roothaan-Hall equations[14], generally given as an eigenvalue problem:

$$(2.2) \quad \mathbf{FC}^{\text{new}} = \mathbf{SC}^{\text{new}}\epsilon$$

where  $\mathbf{C}^{\text{new}}$  are the next orbital coefficient solutions,  $\mathbf{S}$  is the overlap, and  $\epsilon$  are the orbital energies. The Fock matrix  $\mathbf{F}$  is calculated from the previous set of orbital coefficients:

$$(2.3) \quad \mathbf{F} = f(\mathbf{C}^{\text{old}})$$

The amount of similarity of orbitals can be estimated from their overlap:

$$(2.4) \quad \mathbf{O} = (\mathbf{C}^{\text{old}})^\dagger \mathbf{SC}^{\text{new}}$$

and for a single orbital can be evaluated as a projection:

$$(2.5) \quad p_j = \sum_i^n O_{ij} = \sum_v^N \left[ \sum_\mu^N \left( \sum_i^n C_{i\mu}^{\text{old}} \right) S_{\mu v} \right] C_{vj}^{\text{new}}$$

where  $\mu, v$  are orbital indices. The population can then be given by the set of orbitals with the highest projection  $p_j$ . This method can be used for any excited state, with the caveat that the orbital solution will most likely be in the same region as the ground state solution. For a small number of low lying states, this is generally true, and so  $\Delta$ -SCF can be used to calculate a small spectrum of excited states[3]. The method of using this orbital overlap is called the maximum overlap method (MOM).

$\Delta$ -SCF has been shown to be cheap alternative to TD-DFT and other higher level methods, without considerable losses of accuracy in certain cases. Additionally, as the excited state is given as solutions to SCF equations, the gradient of this solution can be given by normal mean-field theory. These gradients would be much cheaper than TD-DFT or coupled cluster methods, and so would be better for any dynamic simulation.

### 2.1.2 Eigenvalue Difference

Another approximation to full response theory would be to eigenvalue difference method. Here there is assumed to be no response of the orbital energies and shapes when interacting with light. This would be recovered from the complete Cassida equation if the coupling elements in the **A** and **B** matrices are set to zero. This gives the difference between the excited state energy and the ground state energy, the transition energy, as just the difference of the orbital energies between the orbital an electron has been excited ( $\epsilon_e$ ) to and the orbital has been excited from ( $\epsilon_g$ ):

$$(2.6) \quad \Delta E = \epsilon_e - \epsilon_g$$

Additionally, transition properties can be calculated by construction transition density matrices from only the ground state solution, needing only a single SCF optimization. Generally, eigenvalue difference methods are not seen as accurate response methods, but can offer a quick and easy initial value[4].

### 2.1.3 Transition Density and Dipole Moments

$\Delta$ -SCF transition properties, such as the transition dipole moment, can be calculated from the SCF solutions for the ground and excited states. The reduced one-particle transition density matrix  $\mathbf{D}^{21}$  can be written as:

$$(2.7) \quad \mathbf{D}^{21} = |\Psi_1\rangle\langle\Psi_2|$$

where  $|\Psi_n\rangle$  is the Slater determinant of state  $n$ , constructed from the set of spin orbitals  $\{\phi_j^{(n)}\}$ . Expressed in terms of the molecular orbitals coefficients  $\mathbf{C}^{(n)}$ , the transition density matrix is given by

$$(2.8) \quad \mathbf{D}^{21} = \mathbf{C}^{(2)} \text{adj}(\mathbf{S}^{21}) \mathbf{C}^{(1)\dagger}$$

where  $\mathbf{S}^{mn}$  is the overlap of the two states. The adjunct of the overlap correspond to Löwdin's normal rules for non-orthogonal determinants [10]. For transition dipole elements, this is:

$$(2.9) \quad \langle \Psi_2 | \hat{\mu} | \Psi_1 \rangle = \sum_{jk} \mu_{jk}^{21} \text{adj}(\mathbf{S}^{21})_{jk}$$

where  $\hat{\mu}$  is the one-electron transition dipole operator, and  $\mu_{jk}$  is the element of this operator corresponding to orbital indices  $j, k$ . The determinant of this overlap, the orbital inner products, can be defined as the inner product of the two states:

$$(2.10) \quad |\mathbf{S}^{21}| = \langle \Psi_2 | \Psi_1 \rangle$$

The general definition of the transition dipole

$$(2.11) \quad \mu^{1 \rightarrow 2} = \langle \Psi_2 | \hat{\mu} | \Psi_1 \rangle$$

can be expressed with this transition density matrix as:

$$(2.12) \quad \begin{aligned} \langle \Psi_2 | \hat{\mu} | \Psi_1 \rangle &= \text{tr}(\hat{\mu} | \Psi_1 \rangle \langle \Psi_2 |) \\ &= \text{tr}(\hat{\mu} \mathbf{D}^{21}) \end{aligned}$$

### 2.1.4 Semi-empirical extensions

A main investigation of this chapter was whether the range of DFT methods that could be used for  $\Delta$ -SCF and eigenvalue difference methods could be extended by using tight-binding methods to predict transition properties. This mainly focused on the recently published GFN-xTB method, parameterized by the Grimme group [7]. This method has been parameterized for geometries, frequencies and non-covalent interactions, and uses an extended version of Hückel theory. The name GFN-xTB is acronym for "Geometries, Frequencies, Non-Covalent - eXtended Tight Binding". This method was chosen for two reasons. The first being that the GFN-xTB method was already implemented in the QCORE package. This significantly reduced the amount of effort required for this project. Additionally, there would be other users and developers who would help with implementation of this new method. Second is that a similar method has already been published that calculates transition properties, the precursor to the GFN-xTB methods. This is the sTDA-xTB method [6].

#### 2.1.4.1 sTDA-xTB

sTDA-xTB ("simplified Tann-Danoff Approximation - eXtended Tight Binding") is another method in the family of xTB methods developed by the Grimme group, and is parameterised for transition properties. The accuracy in calculating transition energies with this method is very good, with the error to high-level results being around 0.3 - 0.5 eV.

Similar to other xTB methods, the sTDA-xTB method is a tight-binding method that uses empirically fit parameters and a minimal basis set. It was trained on a test set of highly accurate coupled cluster and density functional theory excitation energies, as well as atomic partial charges for inter-electronic interactions.

Unlike other xTB methods, coefficients in the basis set for sTDA-xTB is dependent on the D3 coordination number. This makes basis functions far more flexible, which would usually be achieved in with fixed basis functions by using diffuse or other additional orbitals in the basis set. Additionally, it uses two sets of parameterized basis sets - a smaller valence basis set (VBS) and an extended basis set (XBS). Whilst this reduces the cost of having larger basis sets, it makes the gradient calculations of transition properties much more difficult.

The two basis sets are used to construct formally similar Fock matrix elements, however in practice they use different global parameters. The core Hamiltonian is similar to other DFTB methods that use a self-consistent charge (SCC) method, as opposed to an SCF method, to obtain molecular orbital coefficients. It is given by:

$$(2.13) \quad \langle \psi_\mu | H^{\text{EHT, sTDA-xTB}} | \psi_\mu \rangle = \frac{1}{2} \left( k_\mu^l k_\nu^{l'} \right) \frac{1}{2} \left( h_\mu^l h_\nu^{l'} \right) S_{\mu\nu} - k_T \langle \psi_\mu | \hat{T} | \psi_\nu \rangle$$

where,  $\mu, \nu, l, l'$  are orbital and shell indices  $k_\mu^l$  are shell-wise Hückel parameters,  $h$  are effective atomic-orbital energy levels,  $S$  is the overlap,  $k_T$  is a global constant and  $\hat{T}$  is the kinetic energy operator. The charges used in the inter-electronic repulsion function are given by CM5 [11] charges for the XBS Fock matrix. These are calculated using Mulliken charges obtained from diagonalising the Fock matrix with the VBS. The charges for the initial VBS Fock matrix are based on Gasteiger charges [2], modified by the parameterised electronegativities of atoms in the system.

The whole process for determining molecular orbitals can be summarized as:

1. Calculate modified Gasteiger charges for initial guess
  2. Diagonalise Fock matrix in the VBS to get the first set of Mulliken charges
  3. Compute CM5 charges
  4. Diagonalise Fock matrix in the VBS again for final set of Mulliken charges.
  5. Recalculate CM5 charges with this final set, and diagonalize the Fock matrix in the XBS.
- The molecular orbital coefficients from this are then fed to the response theory.

The response theory for this method is based on the previous work in the Grimme group on the simplified Tamm-Danoff Approximation [5]. There are several approximations made between full linear response theory and the sTDA method. First is the Tamm-Danoff approximation, where the B matrix is ignored. The second approximation is to use monopole approximations with

Mataga-Nishimoto-Ohno-Klopman operators instead of explicit 2 electron integrals to calculate matrix elements, as well as neglecting the density functional term.

Transition charges are used to calculate these MNOK integrals. The charge  $q_{nm}^A$ , the charge centred on atom  $A$  given by transition density for the transition of  $n \leftarrow m$ , are computed using a Löwdin population analysis:

$$(2.14) \quad q_{nm}^A = \sum_{\mu \in A} C'_{\mu n} C'_{\mu m}$$

where the transformed coefficients  $C'_{\mu n}$  are given by the orthogonalising the original MO coefficients  $\mathbf{C}$ :

$$(2.15) \quad \mathbf{C}' = \mathbf{S}^{\frac{1}{2}} \mathbf{C}$$

and  $\mu$  is an index that runs over the atomic orbitals (AO).

The operator is the MNOK[12][13][9] damped coloumb function, with different exponents  $y_K$  and  $j_J$  for exchange and coulomb integral respectively. The  $\alpha_x$  parameter is included to recover the amount of Fock exchange mixing in the original matrix element equation, and is a free parameter. These will be discussed in more detail in the next chapter, as they are a crucial part of designing a new response method for chlorophyll systems.

Third is the truncation of single particle excited space that is used to construct the  $\mathbf{A}$  matrix. This reduces the number of elements that need to be calculated, and so reduces the time taken for diagonalisation, whilst also capturing a broad enough spectrum of excitation energies. The sTDA-xTB has many of the same goals as this project, except in one respect, which is the gradient theory. As the sTDA-xTB method still requires constructing and diagonalizing the  $\mathbf{A}$  matrix, albeit with a tight-binding method for molecular orbital coefficients, the gradient of the transition properties would still be difficult to calculate.

## 2.2 Benchmarking

The first step in testing whether a GFN-xTB based  $\Delta$ -SCF method (which we name  $\Delta$ -xTB ) could predict TD-DFT transition properties with decent accuracy was to test a set of small molecules, as well as bacterial chlorophylls from the LHII protein against high-level results.

### 2.2.1 Reference Data and test set

The test set comprised of 109 small molecules. Each system was closed-shell, contained 12 atoms or less, and contained on H, C, N, O and F atoms. The size and relative simplicity of this test set was chosen to minimise any other factors that could cause complication in analysing the results.

For example choosing a consistently correct basis set and functional for the  $\Delta$ -SCF results would have been challenging if we had to include transition metal complexes, as well as if we had to think about CPU walltime. Additionally, the size of these molecules made symmetries much easier to inspect by hand.

Reference data was calculated as the three lowest energy singlet excited states, using EOM-CCSD with an aug-cc-pVTZ basis set. These results were generated using the Gaussian 16 program [1].

### 2.2.2 Small Systems

Transition properties for this test set were calculated using TD-DFT and  $\Delta$ -SCF, both using a CAM-B3LYP functional and aug-cc-pVTZ basis set. The transitions were assigned to the EOM-CCSD results by comparing transition dipoles, energies and the character of the MOs involved in the transitions. Where the symmetries could be assigned, these were also used, however this was not the case for all systems as many were unsuccessful in labelling symmetry or defaulted to a non-Abelain group. Symmetry labelling was also only available for TD-DFT calculations, as these were performed with Gaussian 16.  $\Delta$ -SCF calculations were done with the QCORE program.

The  $\Delta$ -SCF singlet transition is not a correct representation of a true singlet excitation, as this is a superposition of both spin-same  $\alpha \rightarrow a, \alpha$  and spin-flipping  $\alpha \rightarrow a, \beta$  excitations. The spin-purification formula:

$$(2.16) \quad \Delta E_S = 2\Delta E^{i,\alpha \rightarrow a,\alpha} - \Delta E^{i,\alpha \rightarrow a,\beta}$$

was used to correct for the true singlet excitation energy  $\Delta E_S$ .

The results of comparing transition energies and transition dipole magnitudes are shown in figures 2.1 and 2.2.

Overall, the excitation energies calculated with  $\Delta$ -SCF are as accurate at predicting EOM-CCSD energies as TD-DFT. The mean error is 0.35 eV, with a standard deviation of 0.25 eV. This is a marginal improvement on the TD-DFT results, which has a mean and standard deviation of 0.41 eV and 0.27 eV respectively. Transition dipoles were similarly accurate to the reference data, although  $\Delta$ -SCF performs slightly worse in this respect. The mean and standard deviation in the absolute value of transition dipole moment,  $|\mu|$ , was 0.07 a.u. and 0.08 a.u. respectively. For TD-DFT, the mean and standard deviation were 0.03 a.u. and 0.06 a.u. (the atomic unit here being equal to  $ea_0$ ). The outlier circled in figure 2.1 is an ethene dimer system, and shows the inability of  $\Delta$ -SCF to capture a mixed excited state. The two LUMO orbitals in this dimer system are in-phase and out-of-phase combinations of the  $\pi$ -antibonding orbitals, which are very close in energy. The HOMO orbitals are the same on both ethene molecules, being the  $\pi$ -bonding orbitals, which are degenerate in energy. The first excited state is predicted by TD-DFT and EOM-CCSD to be a mix of these two close HOMO-LUMO transitions, however  $\Delta$ -SCF cannot include this mixed

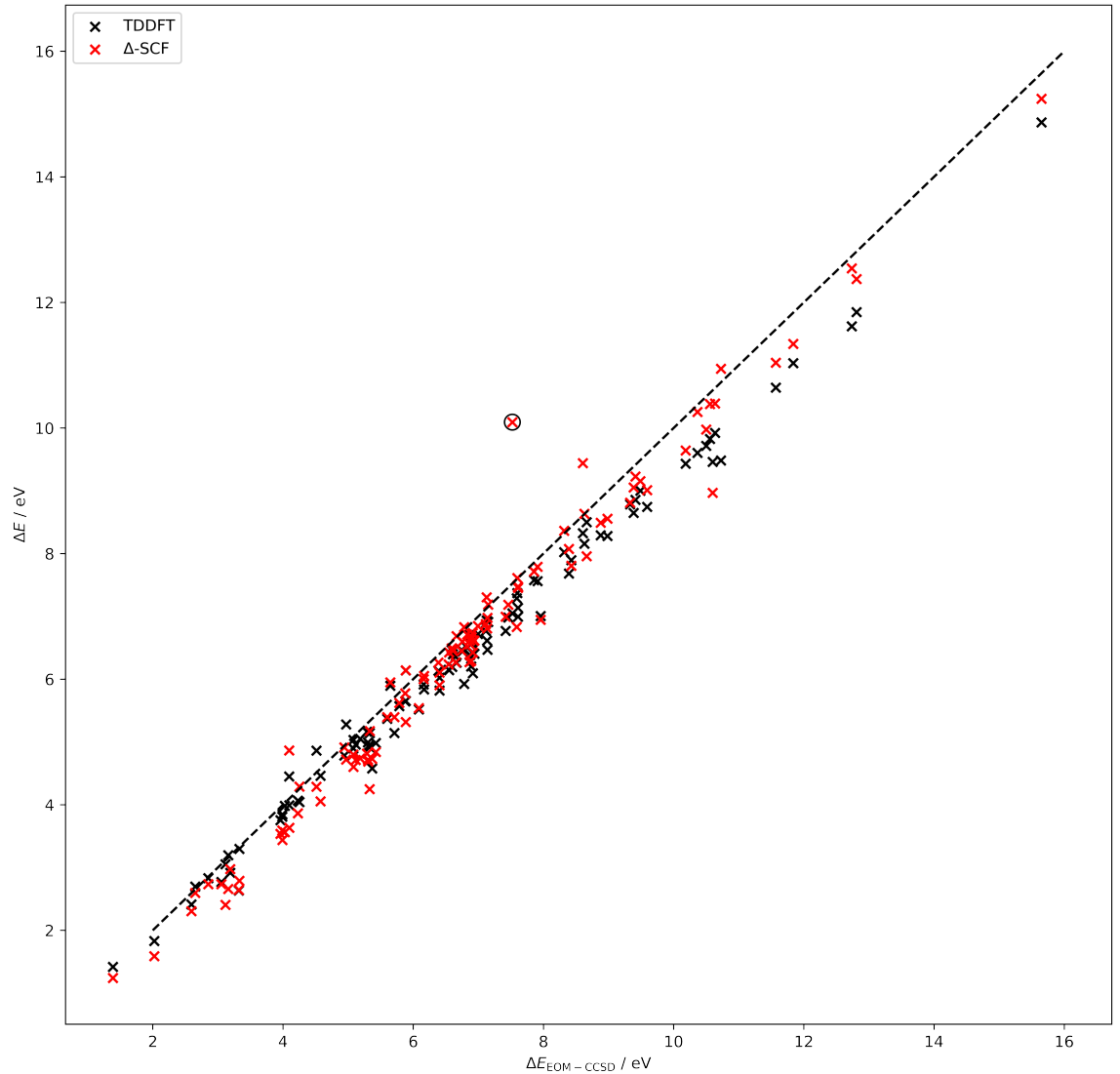


Figure 2.1: Transition energies  $\Delta E$  from TD-DFT (black) and  $\Delta$ -SCF (red) plotted against EOM-CCSD energies, with the line  $y = x$  (dashed) for reference. The ethene dimer outlier has been circled.

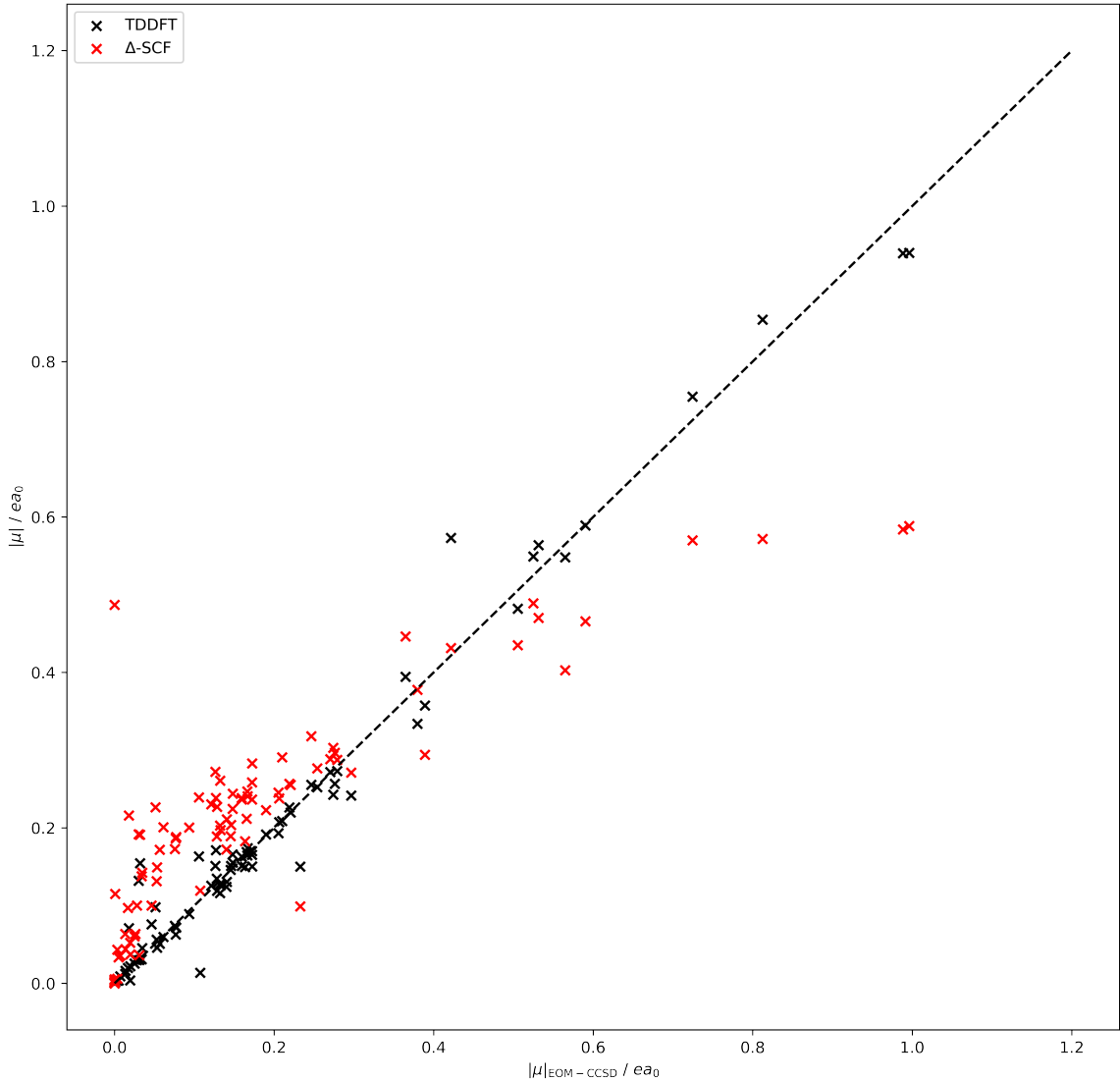


Figure 2.2: Transition dipole magnitudes from TD-DFT (black) and  $\Delta$ -SCF (red) plotted against EOM-CCSD transition dipole magnitudes, with the line  $y = x$  (dashed) for reference.

behaviour.  $\Delta$ -SCF predicts two transitions of 7 eV and 10 eV, whilst TD-DFT and EOM-CCSD predict 7.5 eV.

In summary,  $\Delta$ -SCF can be seen to accurately predict transition properties to a EOM-CCSD level of accuracy with as much success as TD-DFT, except in cases of mixed transitions. It might then be expected a tight-binding method, with good electronic structure treatment, could also be accurate whilst drastically reducing the cost of calculation.

### 2.2.3 Non-orthogonality

There is, however, another caveat with  $\Delta$ -SCF. The ground and excited states, solutions to two separate SCF cycles, will not be truly orthogonal. The Slater determinants  $|\Psi_n\rangle$ , are constructed from the set of orbitals  $\{|\phi_j^{(n)}\rangle\}$  that will be orthogonal within the same state, however the overall states will not be orthogonal to each other, such that the inner product:

$$(2.17) \quad S_{jk}^{21} = \langle \phi_j^{(2)} | \phi_k^{(1)} \rangle$$

will be non-zero. Similarly, there will be a non-zero transition charge:

$$(2.18) \quad q^{21} = \langle \Psi^2 | \Psi^2 \rangle$$

which breaks the origin-independence property of the transition dipole moment. In this way, any transition dipoles that do not have their centre at the origin will have a systematic error based on this overlap and the distance from the origin. For vertical transitions, this transition charge should be zero, and so all transition dipole moments calculated with non-orthogonal  $\Delta$ -SCF would always have this error.

In order to fix this issue, a transformation to symmetrically orthogonalise the two states was applied, which also would preserve as much character of the original states as possible. The transformation is given by:

$$(2.19) \quad |\Psi_{\tilde{v}}\rangle = \sum_v |\Psi_v\rangle \left[ \mathbf{S}^{-\frac{1}{2}} \right]_{v\tilde{v}}$$

where  $\mathbf{S}$  here is a block matrix:

$$(2.20) \quad \mathbf{S} = \begin{pmatrix} 1 & S \\ S & 1 \end{pmatrix}$$

with  $S$  being the overlap value of the two states  $\langle \Psi_2 | \Psi_1 \rangle$ .

It was found that using this method for correcting the non-zero overlap of states, the origin-independence of the transition dipole moment was recovered (see figure 2.2.3). The transition

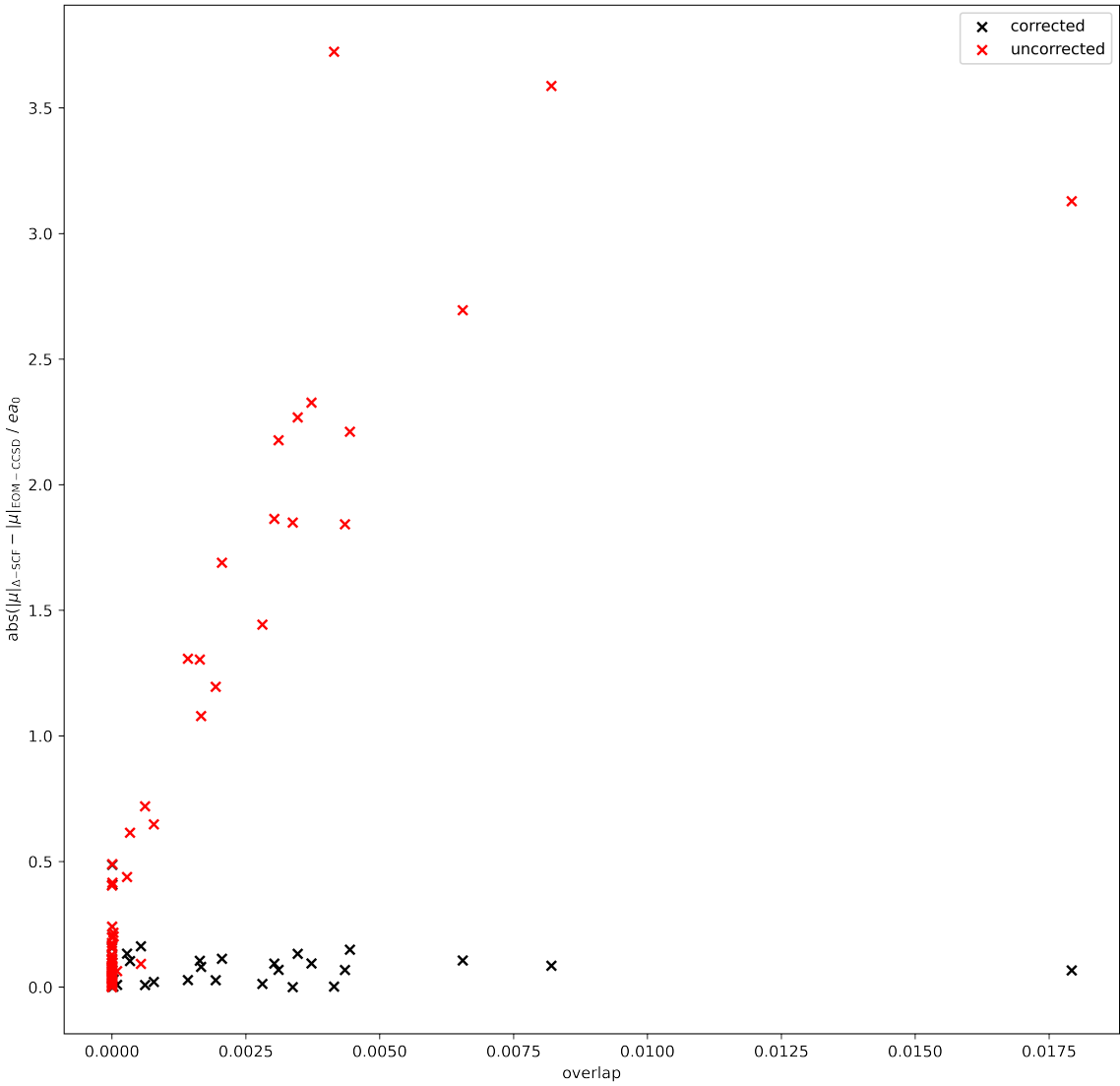


Figure 2.3: The absolute value of the error in transition dipole magnitude between  $\Delta$ -SCF and EOM-CCSD, plotted against the  $\Delta$ -SCF overlap of the ground and excited state. All systems were translated by 100 Å in all cartesian axes. Transition dipole magnitudes calculated without any correction are shown in red, whilst those with the symmetric orthogonalisation correction are shown in black.

dipole for each molecule in the test set systems was calculated for molecules translated by 100Å in each of the  $x$ ,  $y$  and  $z$  axes. This would induce an error for the non-orthogonalised states, which has been corrected for in the calculations with the symmetric orthogonalisation. It should be noted that whilst this effect is dependent on how large the overlap may be, and it could be argued that with a small overlap this effect may not be large, having any large translation of the molecule (on the order of hundreds of angstroms) can lead to nonphysical transition dipole magnitudes. In a large protein system, where these distances can be on this scale, this would obviously present a much larger problem than for a vacuum phase small molecule.

#### 2.2.4 LHII Chlorophyll

The accuracy of  $\Delta$ -SCF was also tested on a set of bacterial chlorophyll A (BChla) molecules. These are a much larger and more complex system, and so present a tougher challenge for the  $\Delta$ -SCF method. Additionally, it is a more relevant test for the goal of simulating a whole LHII complex.

As each Bchla is 140 atoms, EOM-CCSD could not be used as the reference method due to resource constraints, so TD-DFT at a PBE0/Def2-SVP level of theory was used instead. The  $\Delta$ -SCF was run with the same density functional and basis set.

$\Delta$ -SCF can be seen to give transition energies to within the accuracy of TD-DFT, such that the variations in transition energy can be said to be due to physical intra-molecular reasons rather than random error from the  $\Delta$ -SCF method.  $\Delta$ -SCF could therefore be used to accurately predict geometry dependent properties.

However, the error in transition dipole magnitudes is larger than that of the small test set. This error is about 0.42 a.u. larger, but without EOM-CCSD or another high-level method, it's unclear whether this error might be from TD-DFT or  $\Delta$ -SCF . Additionally, there is a clear correlation between the transition dipole magnitudes from TD-DFT and  $\Delta$ -SCF , and so whilst quantitative statements cannot be made, qualitative assessments can be confidently made from  $\Delta$ -SCF data.

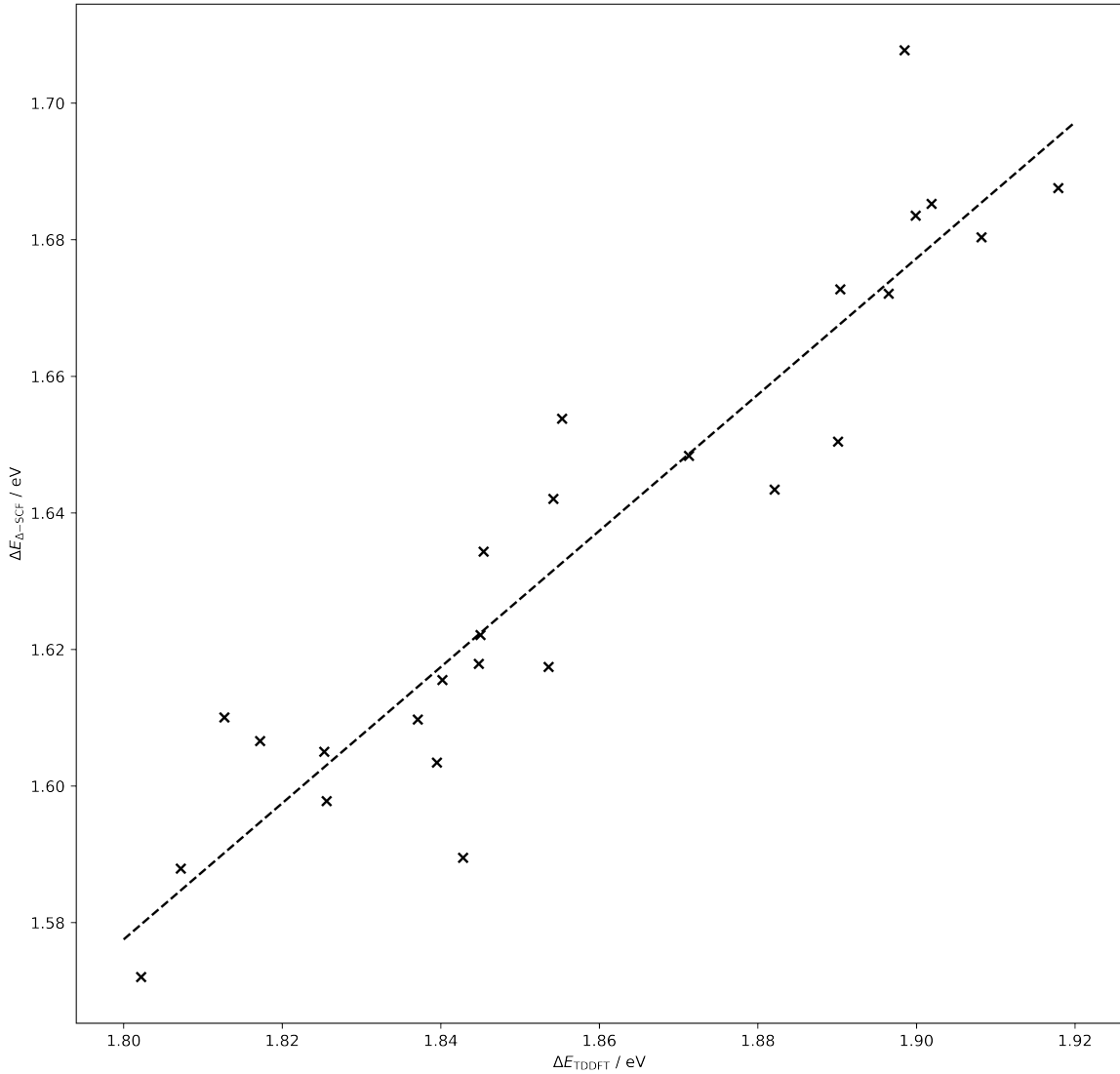


Figure 2.4: The transition energies from  $\Delta$ -SCF for the 26 chlorophyll geometries, plotted against energies from TD-DFT. The line of best fit ( $R^2 = 0.87$ ) is shown as the dashed line.

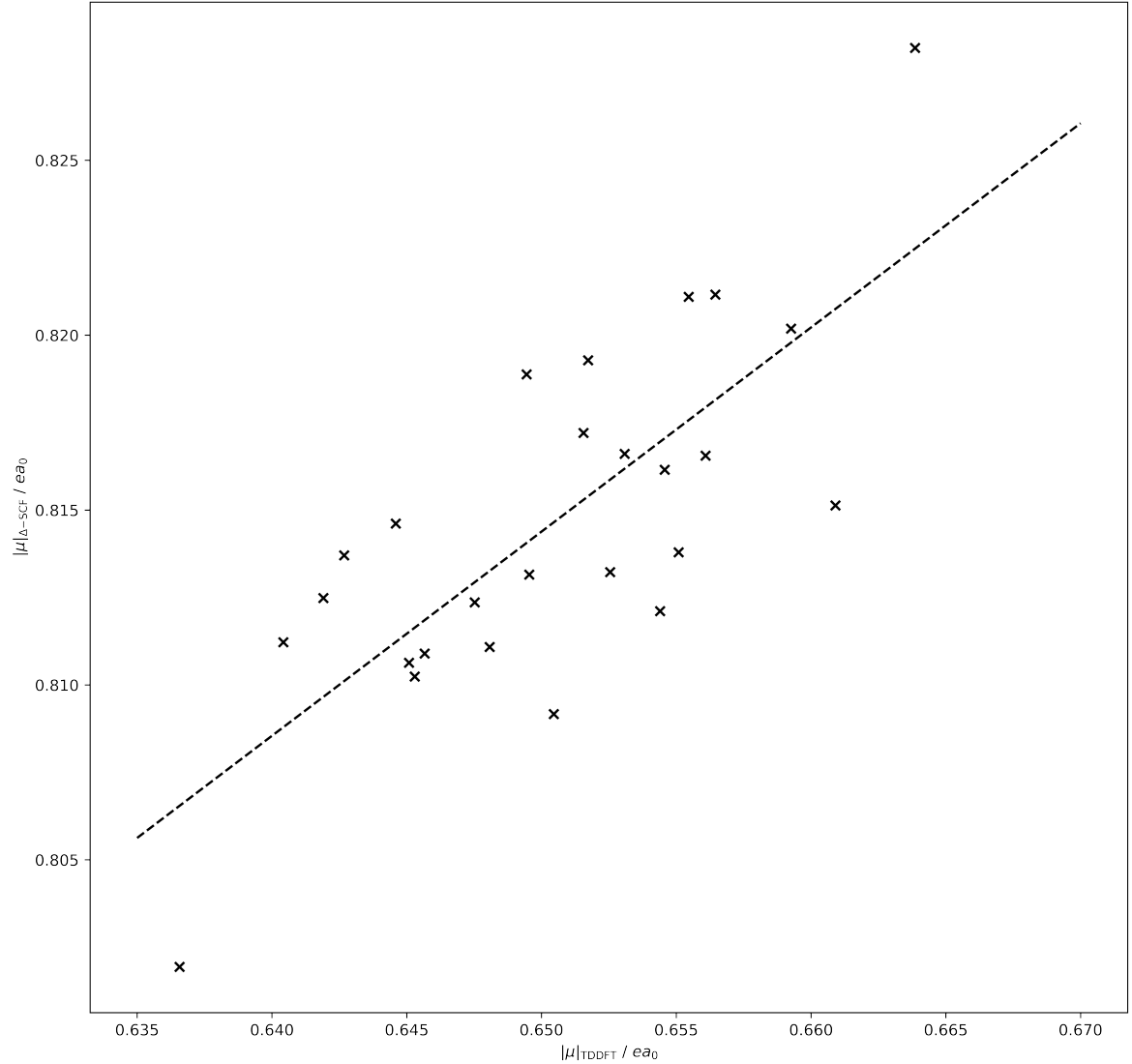


Figure 2.5: The transition dipole magnitudes from  $\Delta$ -SCF for the 26 chlorophyll geometries, plotted against dipole magnitudes from TD-DFT. The line of best fit ( $R^2 = 0.57$ ) is shown as the dashed line.

### 2.2.5 xTB methods

The same benchmarking set was used with the  $\Delta$ -xTB method. The number of methods in the comparison was also expanded to cover a range of approximations in calculating transition properties, including the aforementioned sTDA-xTB method. To include this in the comparison, it was necessary to use the CC2 reference data produced by the Grimme group. Concurrent to this work, the GFN0-xTB method was also implemented in QCORE. This method is similar to the GFN1-xTB method, but excludes any charge dependent terms in its Fock matrix so is not self-consistent. This method therefore only uses a single diagonalisation, with orbital solutions being the same for both ground and excited state. A transition energy from  $\Delta$ -SCF with this method would functionally be the same as an eigenvalue difference, and this was included in the benchmarking to test whether it would be a possibility for predicting transition properties. Also included in this benchmarking is using the eigenvalue differences from sTDA-xTB, given by the `xtb4stda` program, to observe how much improvement to transition properties is caused by the sTDA procedure. `xtb4stda` is the first of two programs that runs a version of xTB, providing molecular orbital coefficients and energies for the sTDA program to then use to calculate the transition properties.

All methods included were:

- High level TD-DFT, with a range separated functional CAM-B3LYP and a aug-cc-pVTZ basis set.
- Lower level TD-DFT, with a PBE0 functional and smaller Def2-SVP basis set.
- $\Delta$ -SCF with CAM-B3LYP/aug-cc-pVTZ.
- $\Delta$ -SCF with PBE0/Def2-SVP.
- linear response with GFN1-xTB and GFN0-xTB.
- $\Delta$ -SCF with GFN1-xTB and GFN0-xTB, named  $\Delta$ -xTB .
- Full sTDA-xTB.
- sTDA-xTB eigenvalue difference.

The results are shown in fig-2.2.5.

These results are discussed in more detail in 2.2.5.2, however it's quickly seen that  $\Delta$ -xTB as well as linear response GFN-xTB is inaccurate at predicting excitation energies. A leading source of error that hasn't been discussed in much detail so far is the assignment of transitions between different methods. A known problem of  $\Delta$ -SCF methods is that the excited state SCF cycle may not converge to the correct state, or it might collapse back to the ground state. This could be seen in the symmetry of the excitation, as if the TD-DFT,  $\Delta$ -SCF and CC2 states have converged to

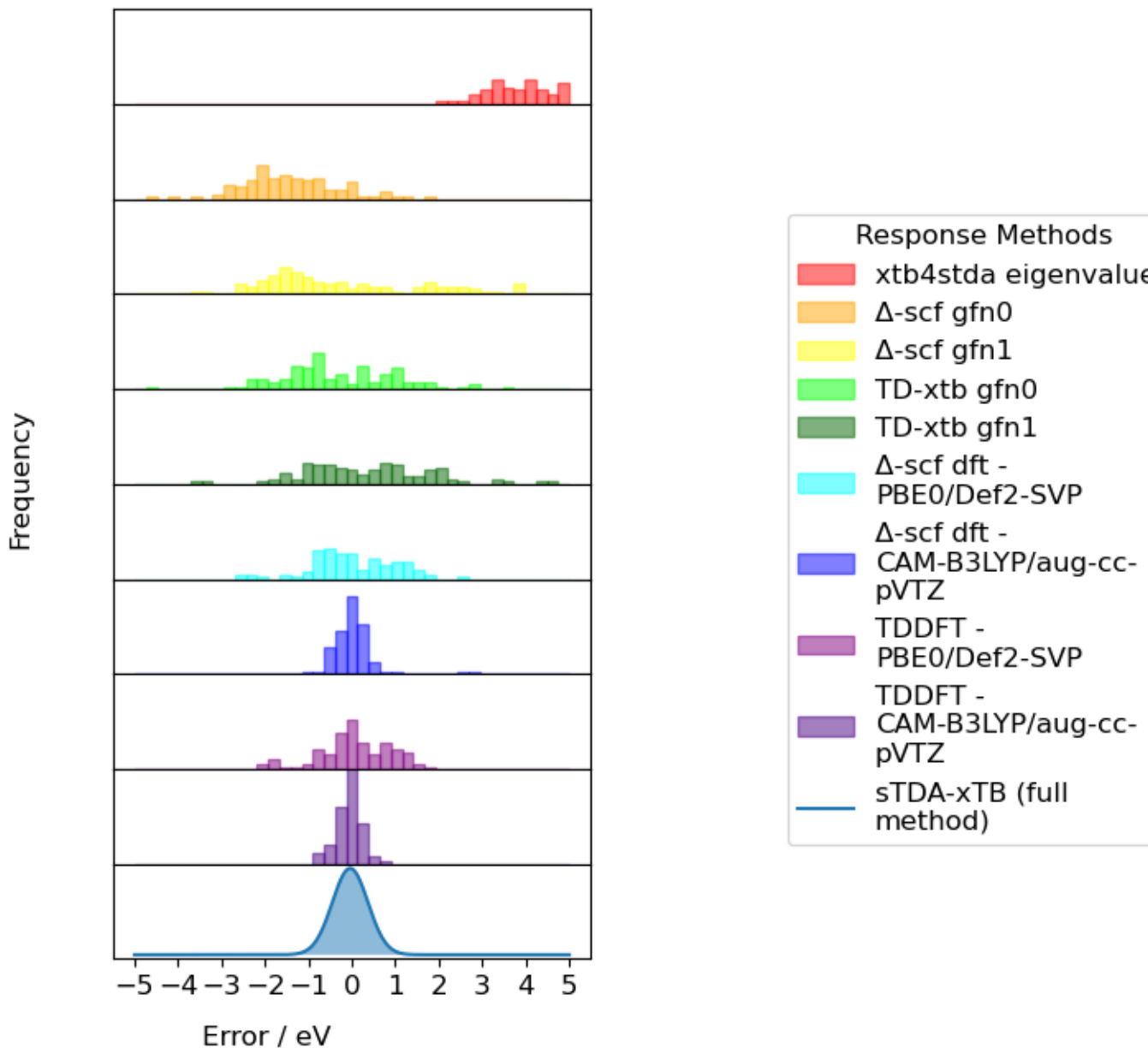


Figure 2.6: The errors of several levels of theory at predicting CC2 transition energies.

different states they would have different symmetries of transition. The benchmarking discussed above used symmetry labels to assign TD-DFT transitions to EOM-CCSD, but as noted earlier this was not always possible, and assigning symmetry labels to  $\Delta$ -SCF was not possible. Instead, transition dipole orientations and plots of MOs were used as a proxy. This would not be possible in this case for two reasons. First is the valence basis set for the  $\Delta$ -xTB calculations are very different to those used in DFT. Second is that this information was not available for the CC2 data, however the symmetry labels were. Additionally, inspecting the symmetry is very time-consuming and can not be automated. Every new method that would be added to the benchmarking would have to have every molecule individually inspected to make sure the symmetry of each transition was correct. Assigning symmetry to  $\Delta$ -SCF results was investigated, but was not a straightforward implementation.

#### 2.2.5.1 Post-SCF Assignment of Symmetry

Considering symmetry is a common thread in many parts of electronic structure theory. It appears in normal mode analysis, wavefunction analysis and assignment of electronic transitions. For this project, assigning symmetry to the transitions for  $\Delta$ -SCF would require assigning symmetry to the MOs and overall wavefunction of a molecule. Broadly speaking, most electronic structure codes have two choices in assigning symmetry to orbitals - either all of the SCF code will treat symmetry from the outset, or nothing is assigned in the SCF code and assignment will happen post-SCF. Both these approaches have benefits and drawbacks. The first method allows the symmetry to be given at any point in the SCF procedure, and allows the Hamiltonian to be organized into a block diagonal matrix. This can be useful when solving for a large basis set or large system as the matrix diagonalisation can be partitioned and parallelised over several cores or nodes on a cluster computer. However, this works best if the system is highly symmetric, which is often not the case when treating unoptimized systems, such as those from a molecular dynamics simulation, and is definitely not the case when looking at biological systems. The second approach, assigning symmetry after the SCF cycles, doesn't fix these drawbacks, but it does allow for codes which originally didn't have symmetry assignment to be extended without rewriting SCF code. The obvious drawback of doing assignment post-SCF is that symmetry can't be utilized during the SCF procedure. The second approach was opted for, as this was the easiest to implement in QCORE. The open source library libmsym was used for point group assignment routines and finding the symmetry adapted linear combination of atomic orbitals. The steps for assigning orbital symmetry is as follows:

1. Determine the point group of the molecule, from the atomic positions
2. Setup the atomic orbitals in the libmsym representation.

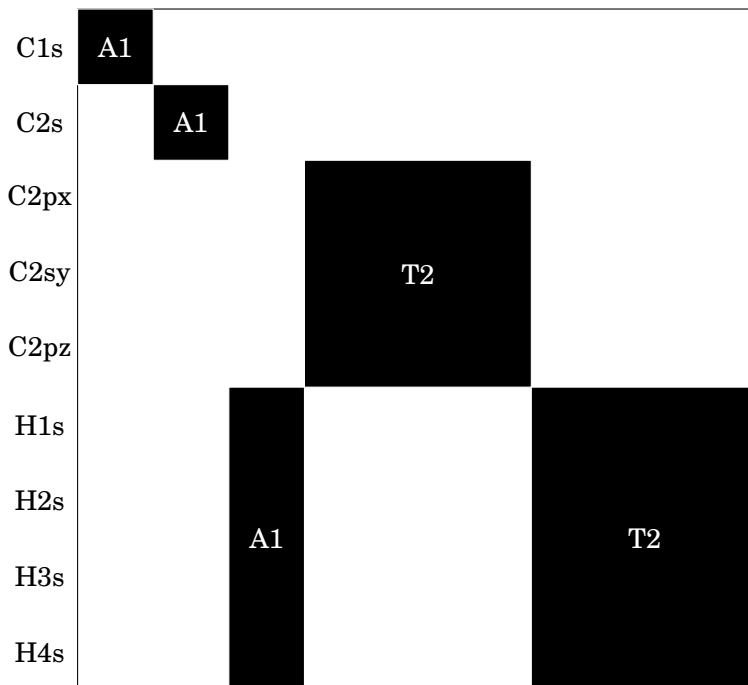


Figure 2.7: A breakdown of the symmetry orbitals in STO-3G methane into the subspaces present in the  $T_d$  point group.

3. Get the symmetry adapted linear combinations (SALCs) of atomic orbitals for each subspace. These subspaces are the groups of symmetries that can be found in the point group of the molecule.
4. The SALCs can then be used to construct the transformation matrix  $T$ .
5. Assign the one electron molecular orbital (MO) for these subspace characters with the symmetry adapted linear combinations.
6. Multiply the one electron MO symmetries together to find the symmetry of the overall wavefunction.

This procedure was implemented and tested on methane with a minimal STO-3G basis set. It was found that this could accurately assign the MOs and overall wavefunction of methane the ground state.

To assign a label to each molecular orbital, we looked at the character of each orbital in all subspaces. This required transforming the molecular orbital coefficients  $\mathbf{C}$  into the each subspace  $A$  by using the transformation matrix  $\mathbf{T}$ :

$$(2.21) \quad \tilde{\mathbf{C}}_A = \mathbf{T}_A^T \mathbf{SC}$$

and then summing the coefficients to obtain the character  $P_A$ :

$$(2.22) \quad P_A = \sum_v |\tilde{\mathbf{C}}_{A,\mu\nu}|$$

where  $\mu, \nu$  are indices for the atomic and molecular orbitals respectively. The molecular orbital with character equal to 1 in a subspace would then have that symmetry label, and would be a well defined assignment. However in practice it is not so clear cut and so the highest subspace character was taken as the assignment.

the MOs for an optimised methane geometry with an STO-3G basis set was correctly assigned - two occupied orbitals and one unoccupied orbital of A1 symmetry, and three occupied and unoccupied orbitals of T2 symmetry. The overall wavefunction symmetry can then be expressed as the product of all MO symmetries, reduced with the reduction formula:

$$(2.23) \quad n = \frac{1}{h} \sum_R \xi_r(R) \xi_i(R)$$

where  $\xi_r, \xi_i$  are the reducible and irreducible representations respectively,  $h$  is the order of the group and  $R$  is the subspace. This correctly produced the overall symmetries of ground state systems for methane and water.

However the assignment of MOs did not work well for excited states, due to the character from the subspace projection being unclear for many MOs. Additionally was that for non-abelian groups, where there are some degenerate E and T subspaces, this assignment did not work. This is a similar problem to the assignment of symmetry for the TD-DFT and EOM-CCSD transitions in the earlier benchmarking. Often the reduction of ground state wavefunctions gave non-physical answers.

Using symmetry decomposition for the non-abelian point groups and analysis based on the antisymmetric component of the direct products was discussed, however this would create a more open-ended project. Additionally, while this may be a useful feature for testing the benchmarking sets, chlorophyll molecules would be far from symmetric and so this type of assignment could not have been expected to have worked. In total transitions could not be confidently assigned for  $\Delta$ -SCF with this method.

### 2.2.5.2 Implications of Benchmarking Results

After considering this leading error, the assignment of symmetry was based on the previously used inspection of transition dipole orientations and transition density plots, however the difficulty of doing this for the entire range of methods should be noted.

Overall, the  $\Delta$ -xTB method is inaccurate - far too inaccurate to be used as a viable method for transition properties of chlorophyll, or any other system. The range of errors is quite large (3 eV)

and there is also a significant systematic shift of 2 eV present. The DFT methods, both the linear-response and the  $\Delta$ -SCF methods, are still shown to be accurate at predicting excitation energies.

The sTDA-xTB results shows that a tight-binding approach that doesn't use full linear-response can give very accurate results, well within a 0.3-0.5 eV range. Again CAM-B3LYP/aug-cc-pVTZ methods, both the linear-response and  $\Delta$ -SCF, are accurate to within this range as well. There are some outliers in the  $\Delta$ -SCF results, that we attribute to different transitions to excited states, however overall both have a majority of errors within a 0.5 eV range. The PBE0/Def2-SVP methods have a marked decrease in accuracy. Both linear-response and  $\Delta$ -SCF methods perform similarly, and so the leading cause of error is attributed to be the electronic structure method, and not the response method.

The GFN-xTB based methods performed much worse than the DFT methods. There is a relatively small difference between linear-response GFN-xTB and  $\Delta$ -xTB results, again showing that poor electronic structure theory gives poor transition properties.

Both the GFN0- and GFN1-xTB based methods proved inaccurate, and there is a marked drop when using GFN0. The systematic shift in the GFN0- $\Delta$ -xTB method is especially bad. It's concluded from this that a response method based on out-of-the-box GFN-xTB would not be viable.

Overall, the most inaccurate method is the eigenvalue difference methods based orbital energies (eigenvalues of the Hamiltonian diagonalisation) from the sTDA-xTB method. Arguably the sTDA method then makes up a large part of predicting transition properties accurately.

The result that gfn-xtb based methods are not accurate is not unexpected. Tight-binding methods in general are inaccurate at calculating electronic interactions, due to not including a large part of the electronic density. Additionally, they are highly parameterised to the certain systems and properties. Whilst the GFN-xTB methods are better than many other methods in this parameterisation, using a few pair-wise parameters as possible to improve extensibility to systems outside the training set, these parameters are trained on ground state properties and not excited state properties. These parameters are found to be unsuitable for predicting transition properties.

## 2.3 Conclusions and Further Work

The transition properties of a test set of small molecules has been benchmarked with multiple  $\Delta$ -SCF, TD-DFT and high-level methods. It has been shown that DFT based  $\Delta$ -SCF and TD-DFT methods can reproduce the same transition energies and transition dipole magnitudes as EOM-CCSD to within reasonable levels of accuracy. For the set of small molecules, transition energies were predicted with a mean of less than 0.5 eV, and 0.07 a.u. for transition dipole magnitudes.

For a small set of BChla geometries, it was found that the same level of accuracy for transition energy could be found between  $\Delta$ -SCF and TD-DFT, where EOM-CCSD was too expensive to

calculate. The error was well within the range of TD-DFT energy variation, shown in the high correlation coefficient, and so  $\Delta$ -SCF could be reasonably expected to give correct geometry-dependent transition energies. Whilst the accuracy is slightly reduced for transition dipole moments, the appreciable degree of correlation implies that qualitative statements would be valid.

GFN-xTB based  $\Delta$ -SCF methods were found to be far more inaccurate, to the point where it cannot be claimed to be a useful proxy to higher level methods. This is attributed to the different electronic structure theory used, rather than the response methods. Whilst this inaccuracy might be due to incorrect comparisons of transitions, efforts to assign symmetry to  $\Delta$ -SCF transitions proved unsuccessful.

Obvious areas for further work would include investigating more systems and response methods. Many other DFTB methods exist, such as ZINDO and . Additionally, whilst Bchla is present in LHII, the same investigation could be repeated for other types of chlorophyll, such as that from the FMO complex. Additionally, the assignment of symmetry could be revisited.

### 2.3.1 Embedding

As reported in this chapter, the benchmarking results do not include any investigation into how these methods would behave in an embedded system. This is more of an implementation problem than a theoretical problem for the majority of the methods investigated, as many of the programs used do not have the option to include point-charge embedding. However, as implemented in QCORE, all of the DFT methods as well as the GFN1-xTB based methods, could have included embedding effects. This would be important to investigate as embedding effects are important to include for biological systems. However as said not all of the methods used have available implementations with embedding. Both the sTDA-xTB and GFN0-xTB do not have published formalisms for embedding. The former would require a deep investigation into the source code of the two programs that currently make up the only implementation of this method, which while not impossible would represent a major task. The latter however was investigated, and proves a simpler task.

However, as GFN0-xTB proved to be inaccurate for transition properties this is not an important task.

### 2.3.2 Scaling

Whilst the  $\Delta$ -SCF results are promising in terms of accuracy and computational effort, this method may not be well suited for calculating properties that depend on many individual calculations, such as a time dependent property. The main issue is scaling up the volume of calculations that could reasonably be done. All of the semi-empirical methods used in this benchmarking had a CPU walltime in the order of seconds, with very small memory requirements. Additionally, they all could be run on a single core due to the larger overhead of serial calculations compared to

the parallelisable routines - i.e. more time would be spent on running SCF cycles or other code which can only be run in serial, than on constructing the Fock matrices or calculating integral values, which can be done in parallel. The opposite is true for the larger scale DFT calculations. Especially for the large chlorophyll system, the memory requirements were much higher than the semi-empirical methods. For example, using the QCORE implementation, all of the chlorophyll calculations required on the order of  $10^2$  gb of memory, and would take 90 minutes of CPU walltime. This included being parallelised over many cores (although not nodes), all of which adds together to make an expensive calculation. This also means that it is entirely unfeasible to run these calculations on a desktop computer.

This severely limits the volume of calculations that can be reasonably be done with these methods. For the 27 individual chlorophylls used in this investigation, the total amount of walltime would be nearly half a days worth on the available supercomputers. Expanding this to a larger scale study of LHII, which can require up to thousands to hundreds of thousands of calculations, would take weeks or months of computational time. The first drawback then is that a study based on this method would not be repeatable in the time frame of a single project. To discover a flaw or additional property that is needed, and so rerun all the calculations even twice or three times, would take on the order of a year and so either be unfeasible or drastically reduce the ability to test new ideas, given that nothing would be allowed to fail. Another drawback is the lack of ease of use. As all calculations would have to be run on a supercomputer, no small assays could be done on a local machine or desktop computer. This is not a major problem, as many methods are unable to be run on a desktop computer, especially large scale DFT calculations. The problem here is that the sTDA-xTB results, which were all run on a desktop computer, show that it is possible to run these systems on smaller machines. It would be worth exploring whether there are more, similar methods that could also achieve this, as this would allow more researchers to be able to run larger systems without the previously needed expense of time and energy, as well as allow for a quicker turnaround time on assays. Additionally, it would also just allow more calculations to be run.

The reliability, or robustness, of  $\Delta$ -SCF is another issue in scaling up the volume of calculations. As mentioned at a couple of points in this chapter, when calculating the excited state,  $\Delta$ -SCF has the occasional tendency to either converge to an unintentional state, collapse back down to the ground state, or not converge at all. It can be very hard to predict when this will happen (for example some Bchla geometries behave like this whilst others do not, which is hard to explain), and requires several tricks to fix. These include Fock matrix damping, changing parts of the SCF convergence algorithm such as the DIIS procedure, or a step-wise initial guesses, such as using an unphysical half-electron excitation as a starting point for a full electron excitation. To work out which trick is needed, and which systems will need them, requires a trial-and-error approach, and it's never guaranteed that something will work. For getting a time series of a transition property from a whole MD simulation, this is obviously a serious problem that would

---

### 2.3. CONCLUSIONS AND FURTHER WORK

need addressing.



CHAPTER



## CHLOROPHYLL SPECIFIC METHODS

**P**reamble this is a preamble.

### 3.1 The Cassida equation

#### 3.1.1 Approximations to Solutions

#### 3.1.2 MNOK Integrals

### 3.2 Parameterization

#### 3.2.1 Reference Data

#### 3.2.2 Objective Function

#### 3.2.3 Minimization Algorithms

### 3.3 Benchmarking

#### 3.3.1 Transition properties

#### 3.3.2 Potential Energy Surfaces

#### 3.3.3 Absorption Spectra

### Excitation Energies correlation

	<b>PBE0</b>	<b>dscf</b>	<b>eigdiff</b>	<b>camb3</b>
<b>PBE0</b>	1	0.915415	0.930766	0.952334
<b>dscf</b>	0.915415	1	0.846607	0.863979
<b>eigdiff</b>	0.930766	0.846607	1	0.925034
<b>camb3lyp</b>	0.952334	0.863979	0.925034	
<b>BLYP</b>	0.730346	0.637576	0.606743	0.6376

Figure 3.1: correlations of energies

Transition Dipole Magnitudes correlation				
	PBE0	dscf	eigdiff	camb3lyp
PBE0	1	0.5891	0.566434	0.762861
dscf	0.5891	1	0.977046	0.800859
eigdiff	0.566434	0.977046	1	0.773252
camb3lyp	0.762861	0.800859	0.773252	1
BLYP	0.0832043	-0.0344407	-0.0098512	0.0500000

Figure 3.2: correlations of transition dipole moments

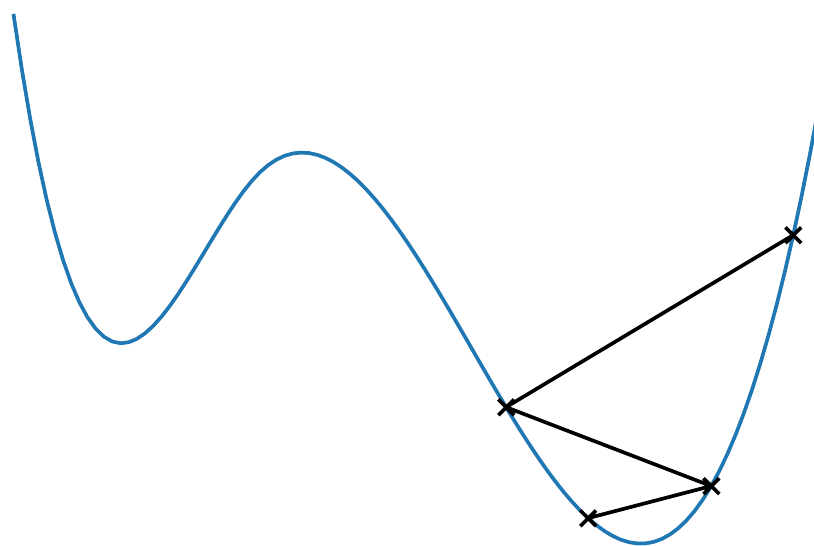


Figure 3.3: Nelder-mead

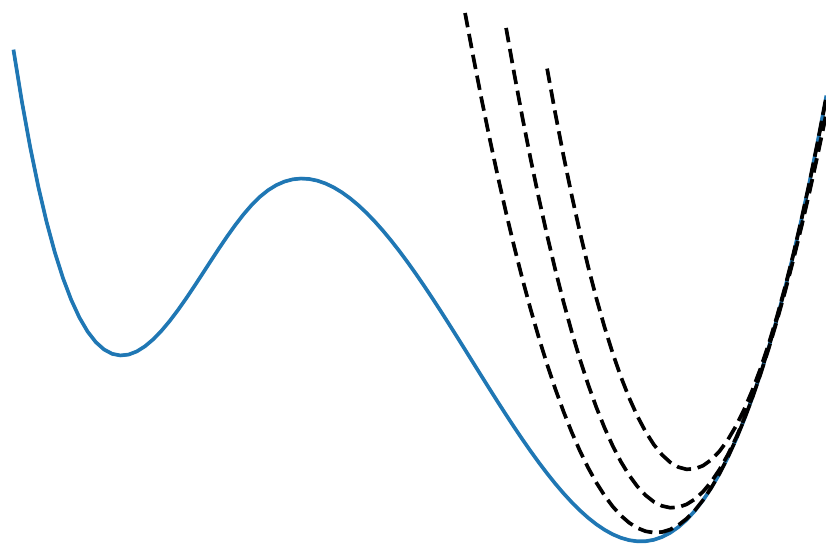
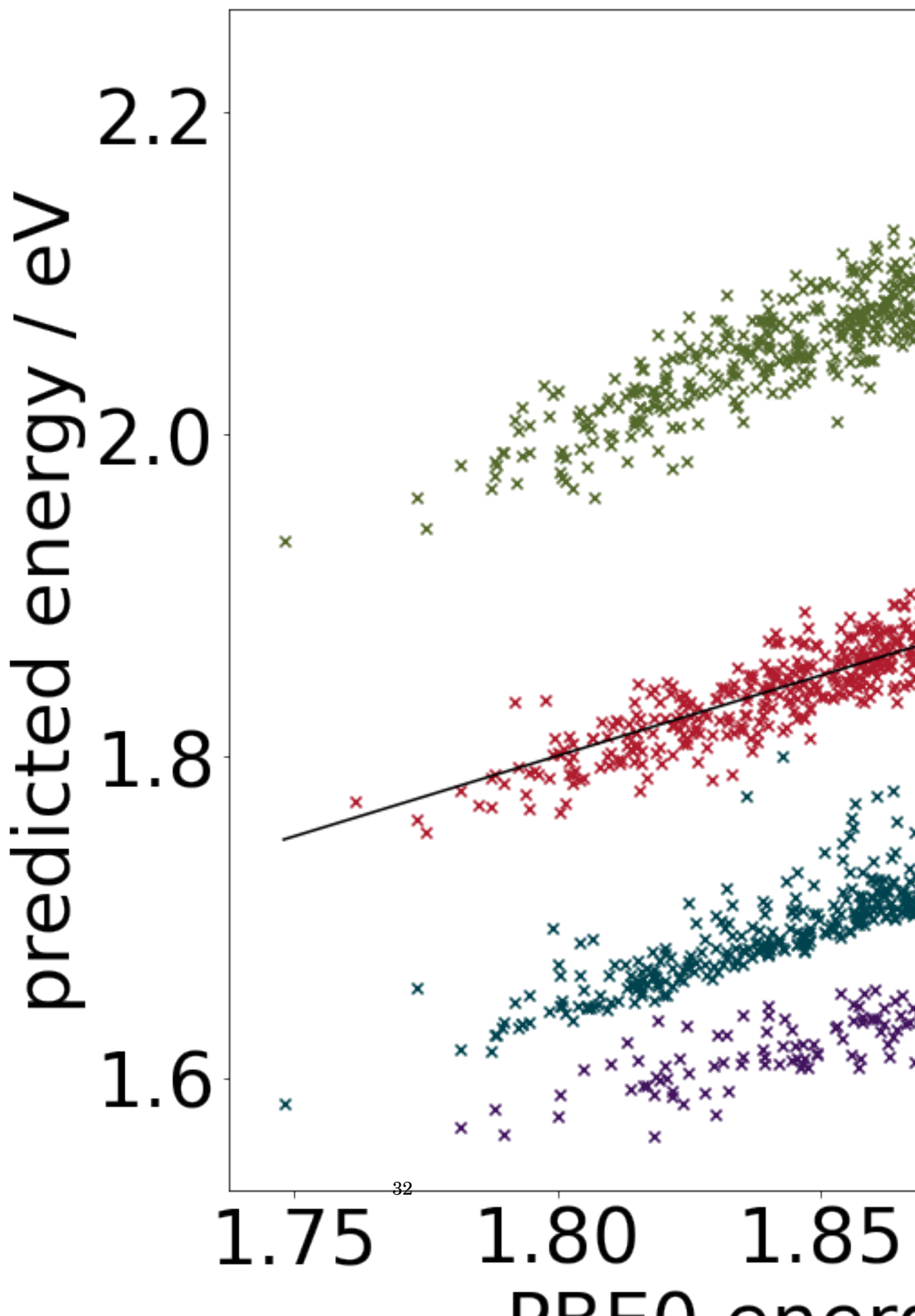
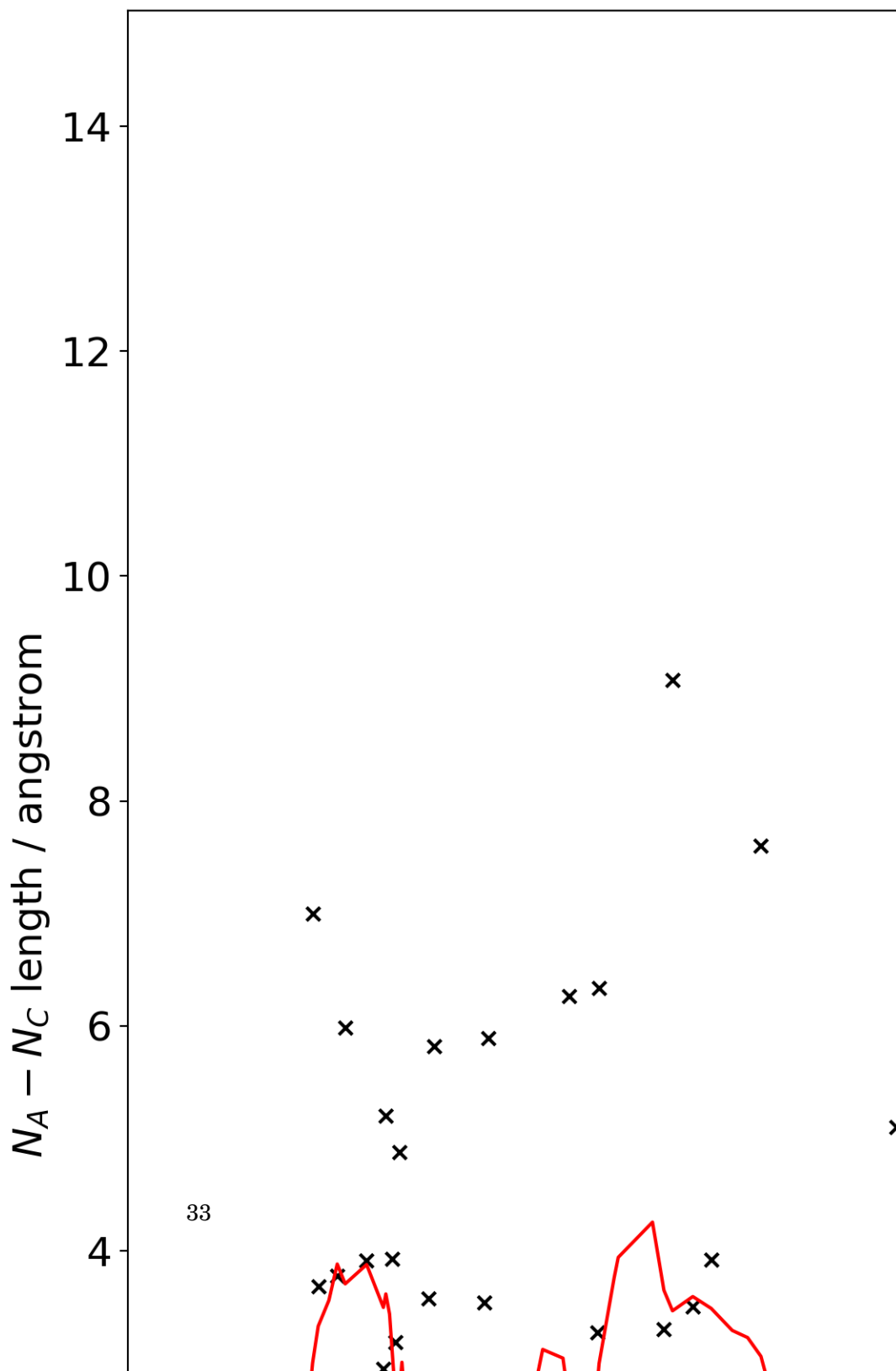


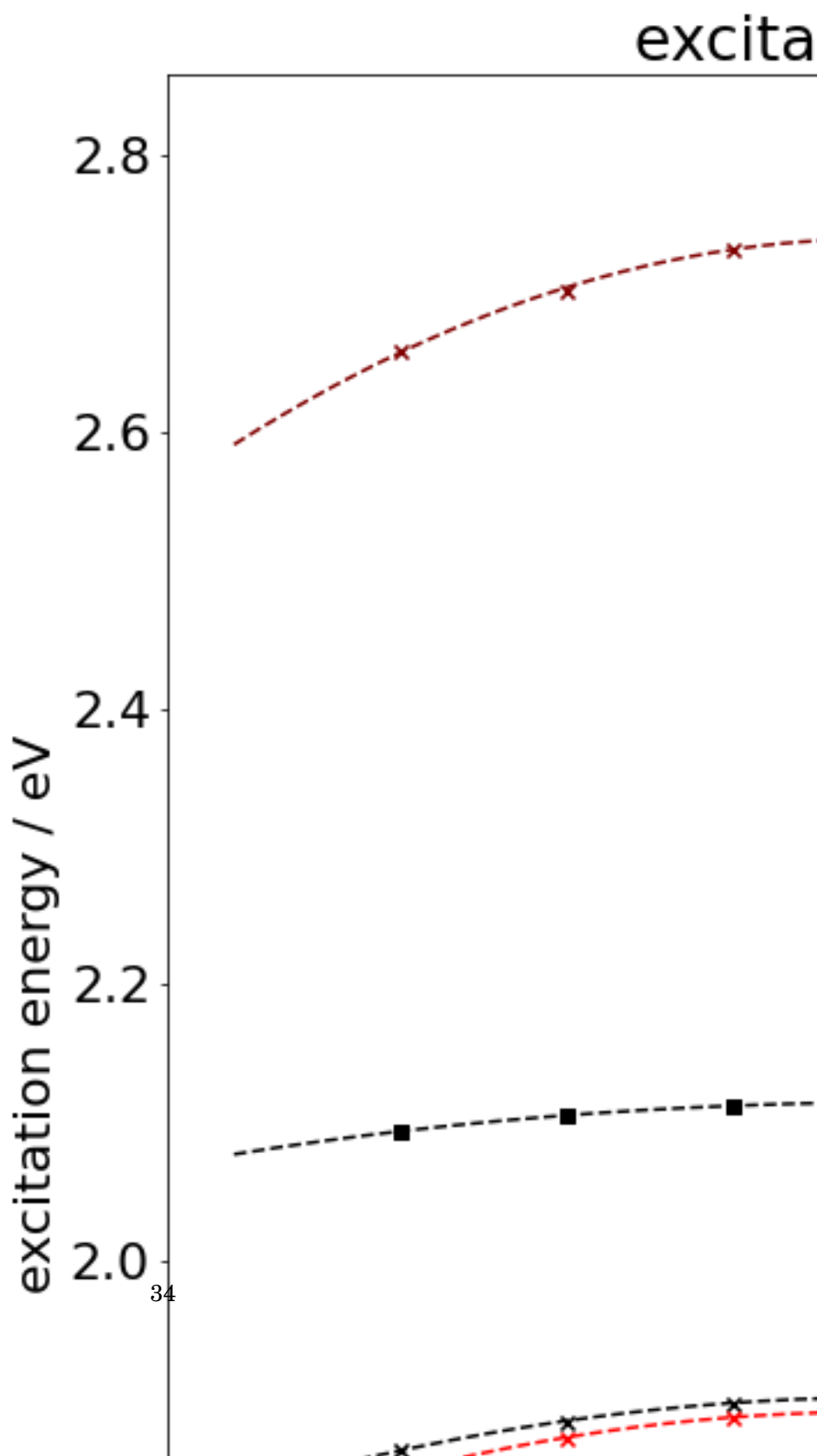
Figure 3.4: SLSQP

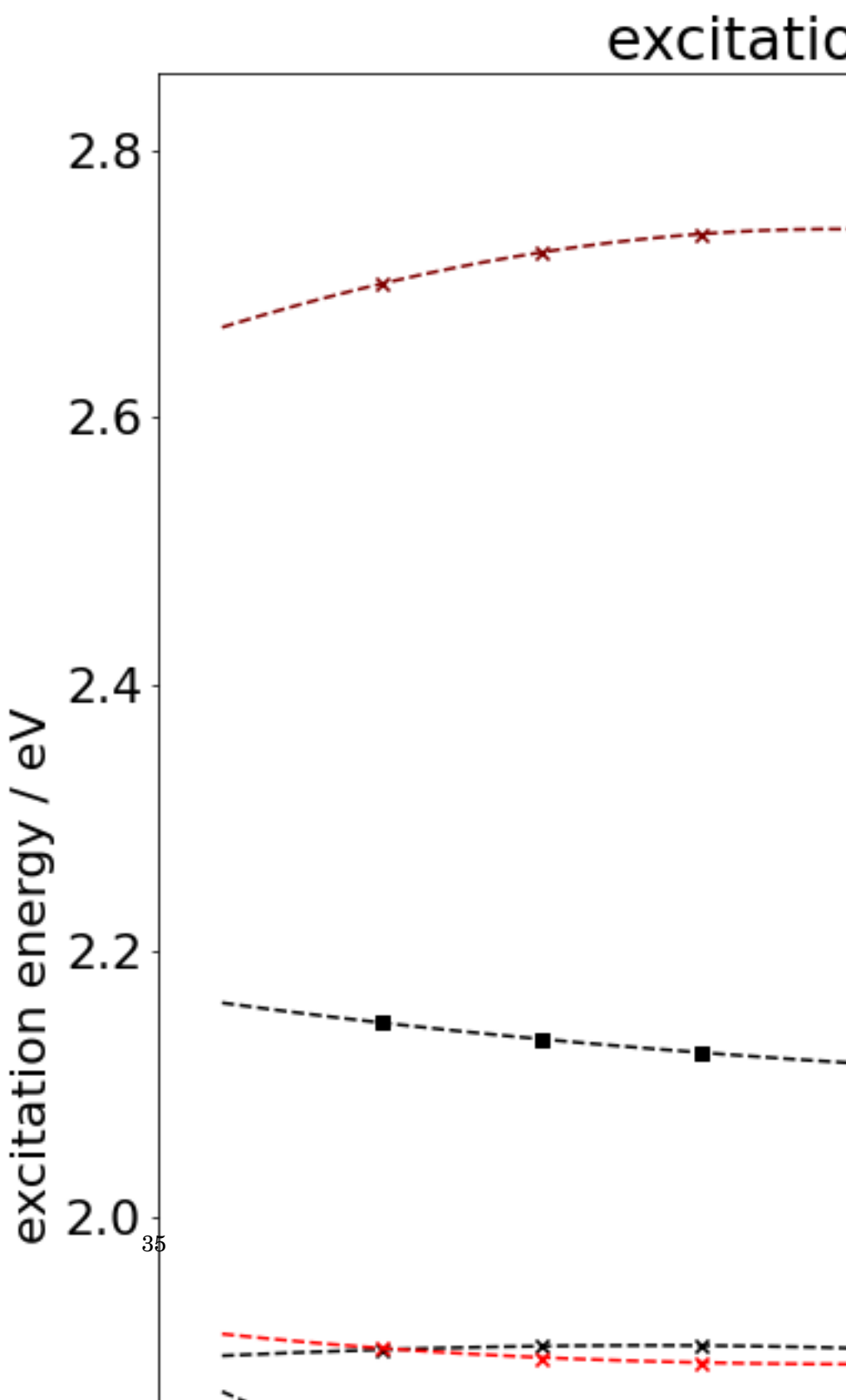
$y_K$	1.0
$y_J$	1.0
$a_x$	1.0

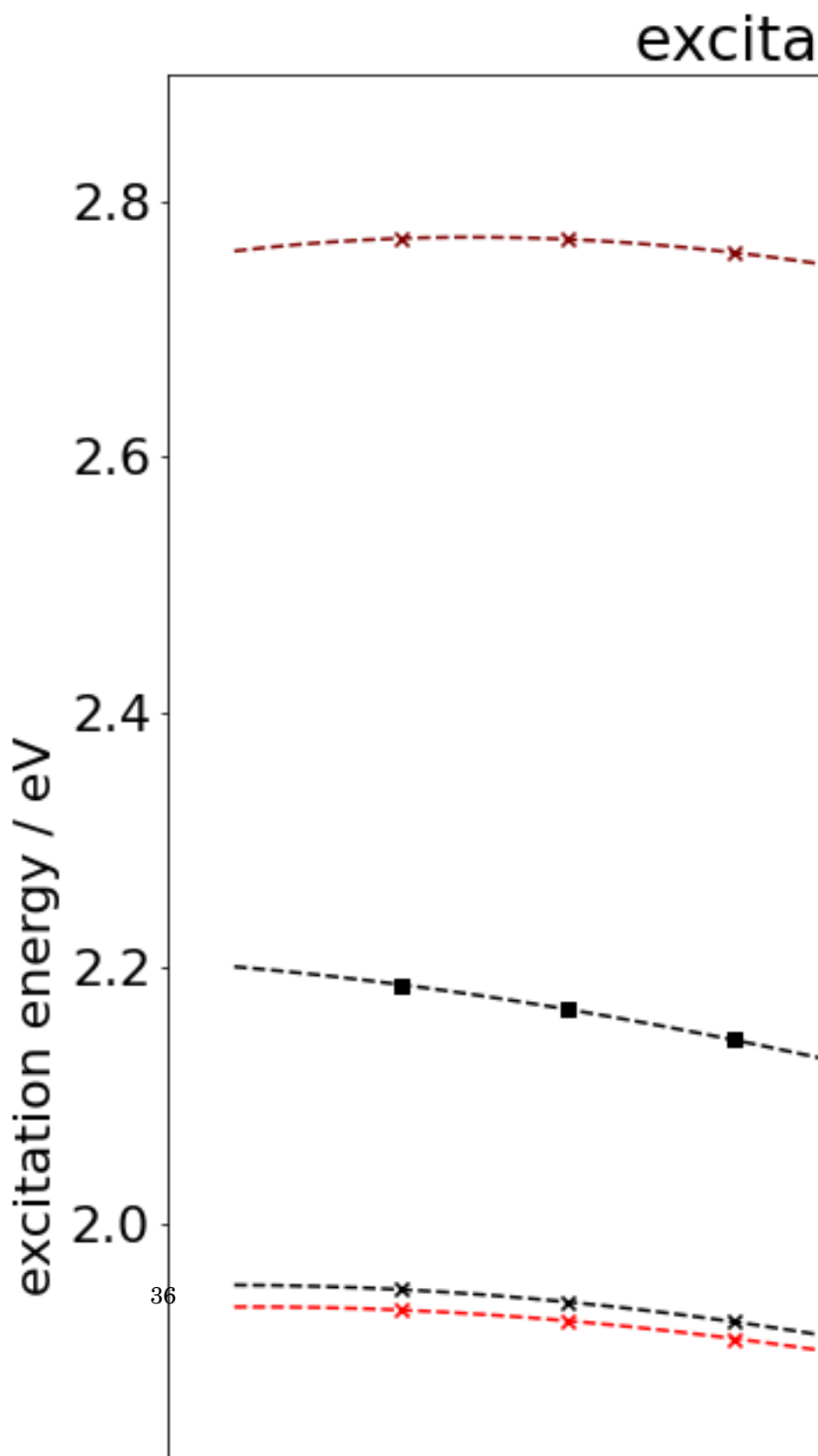
Figure 3.5: optimized parameters from SLSQP procedure.

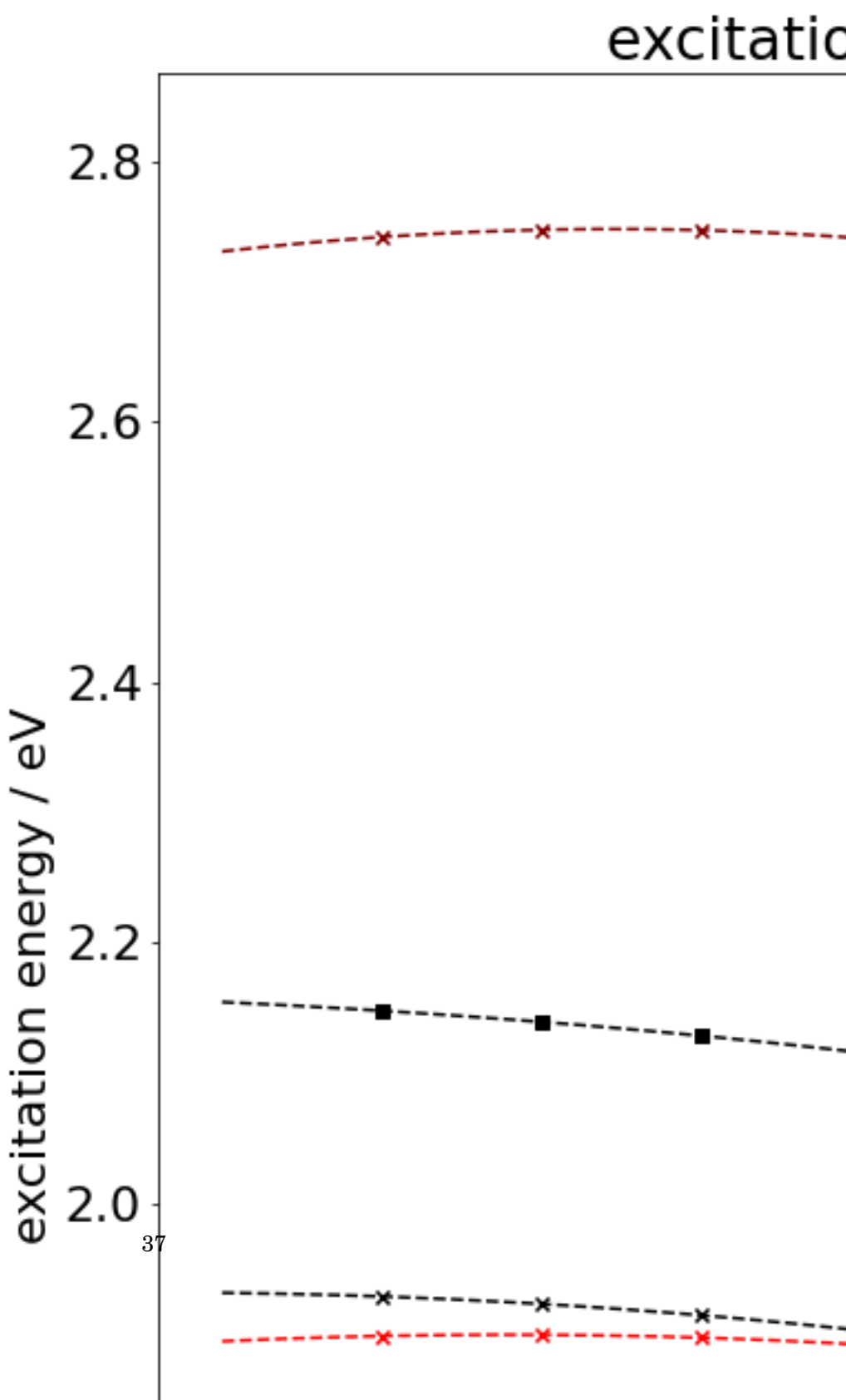


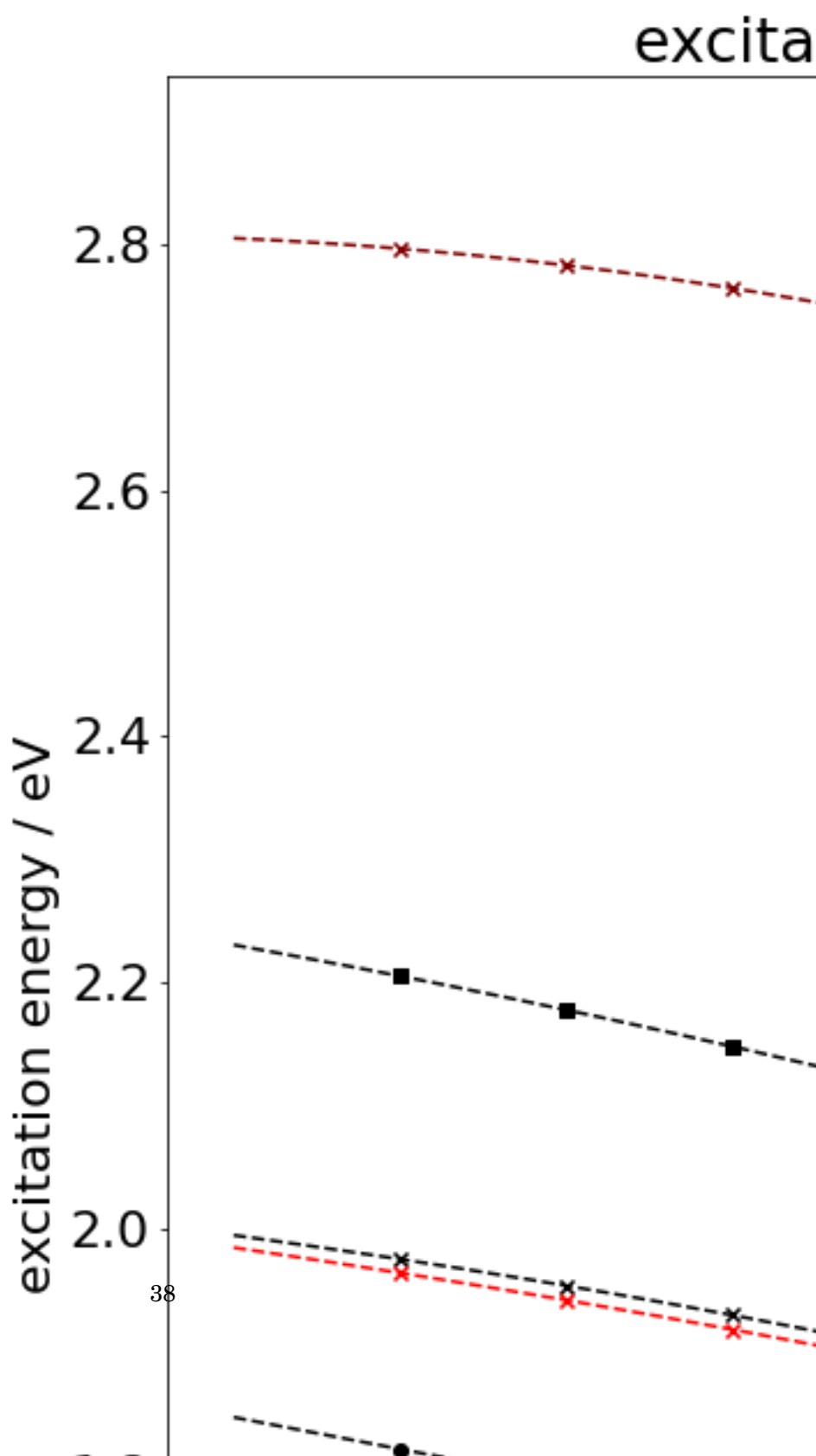


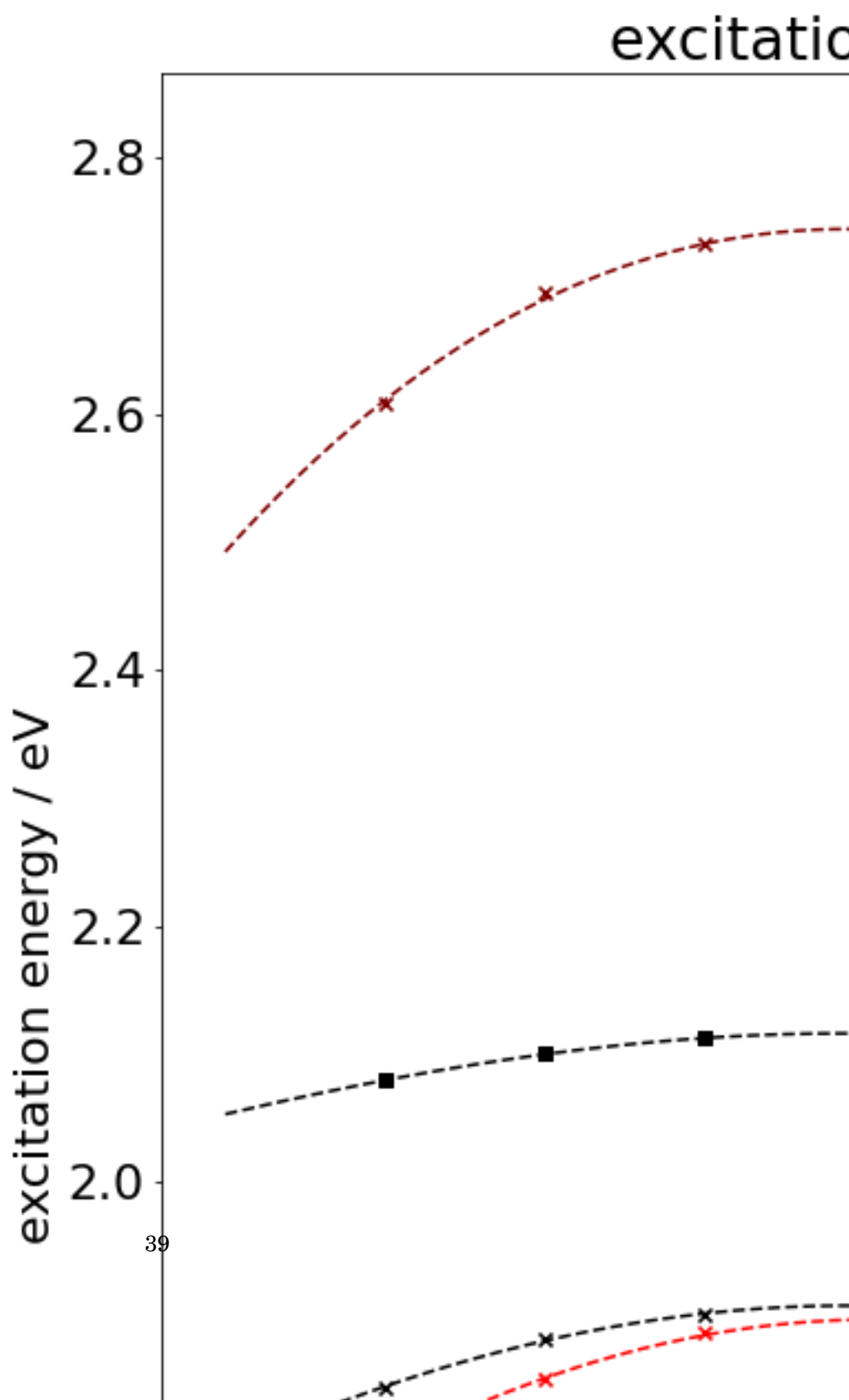


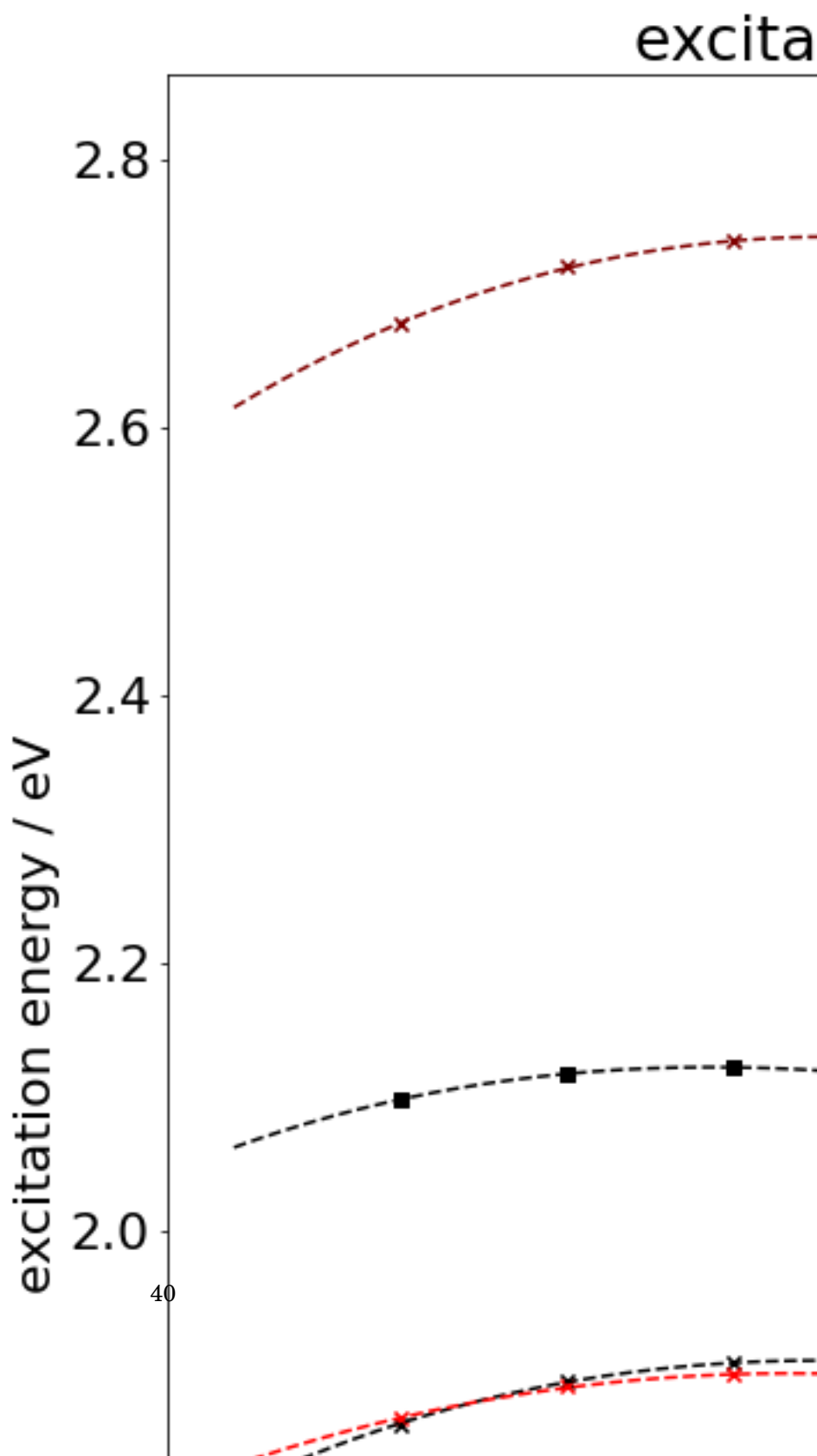


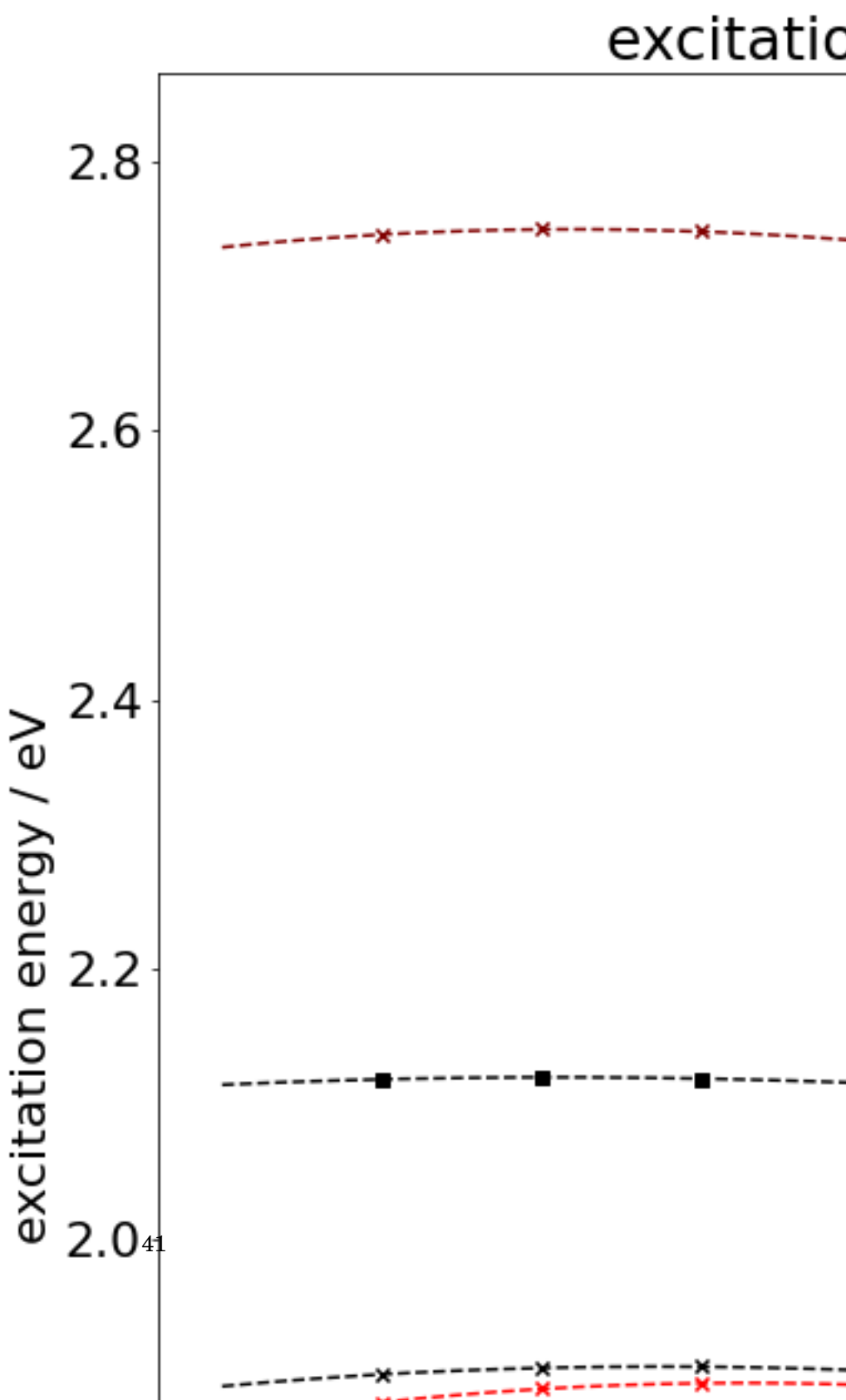


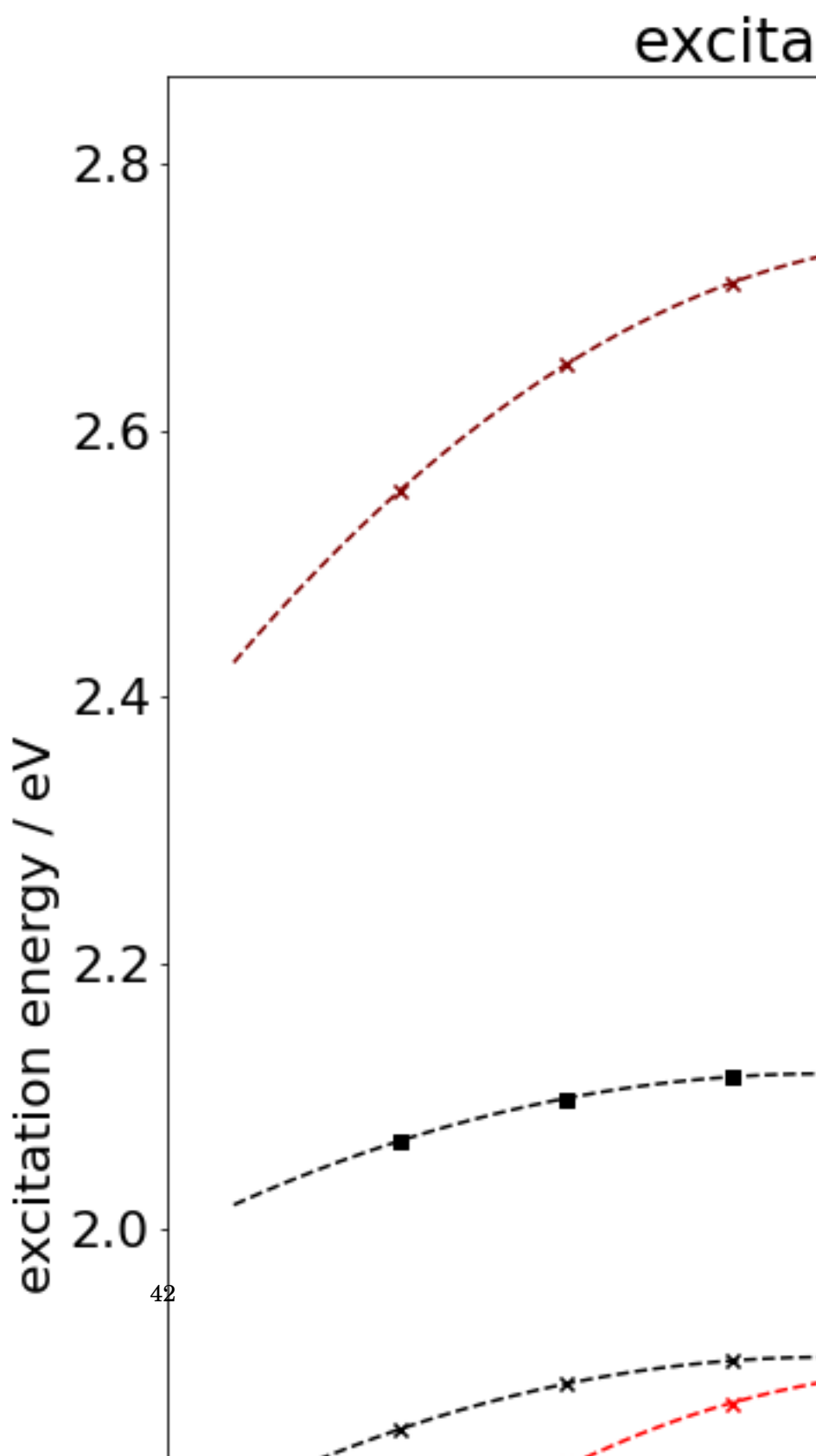


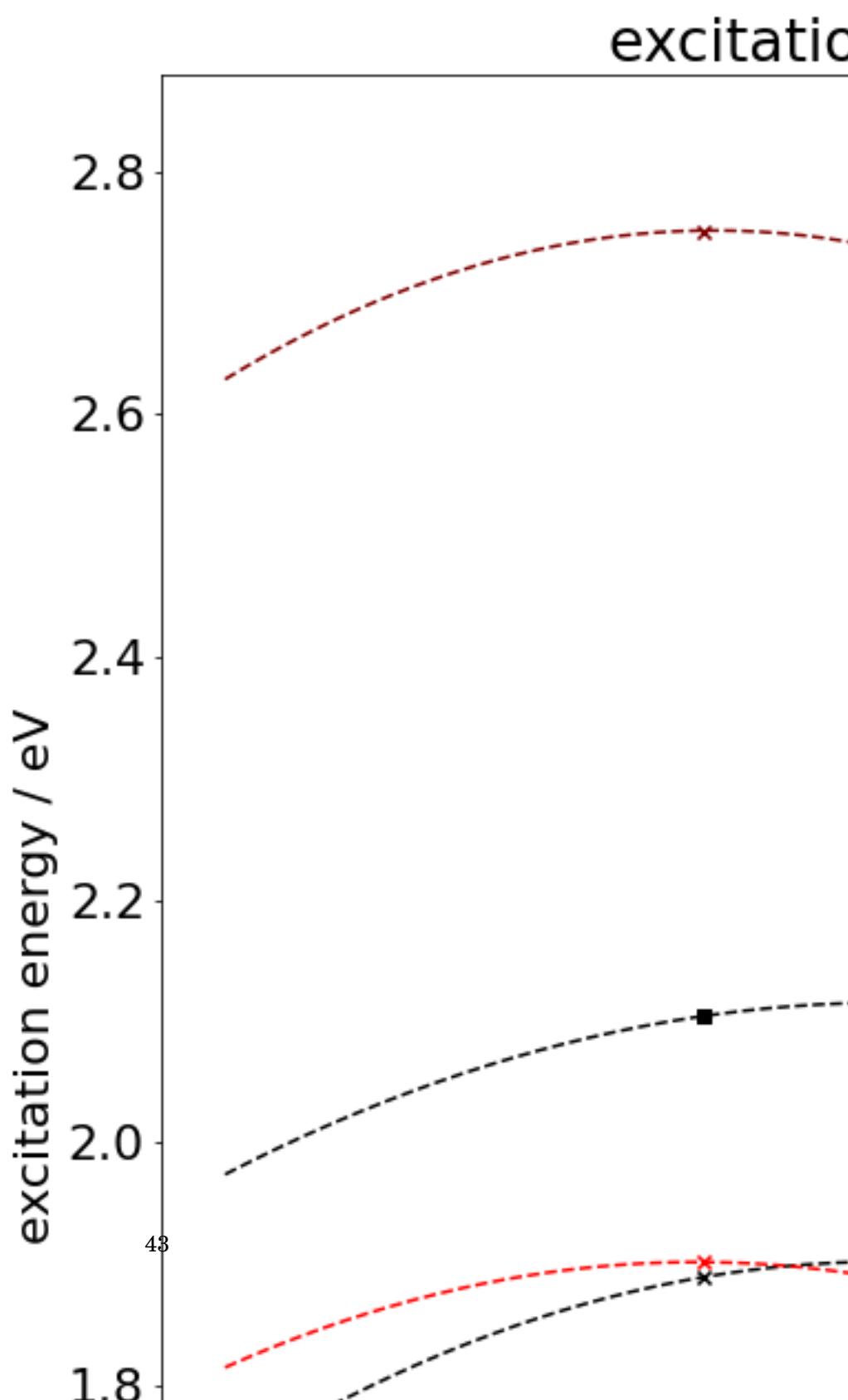


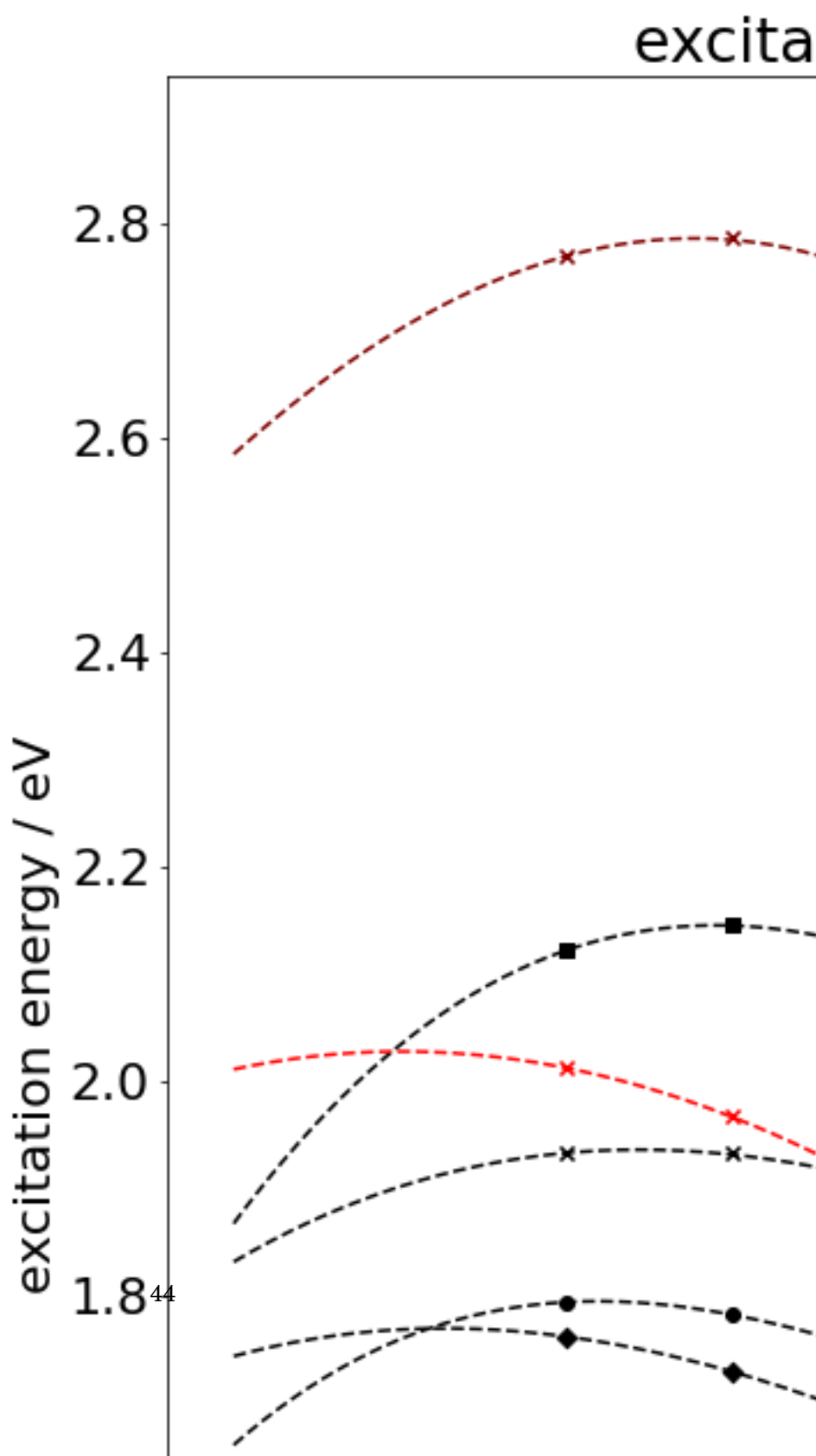










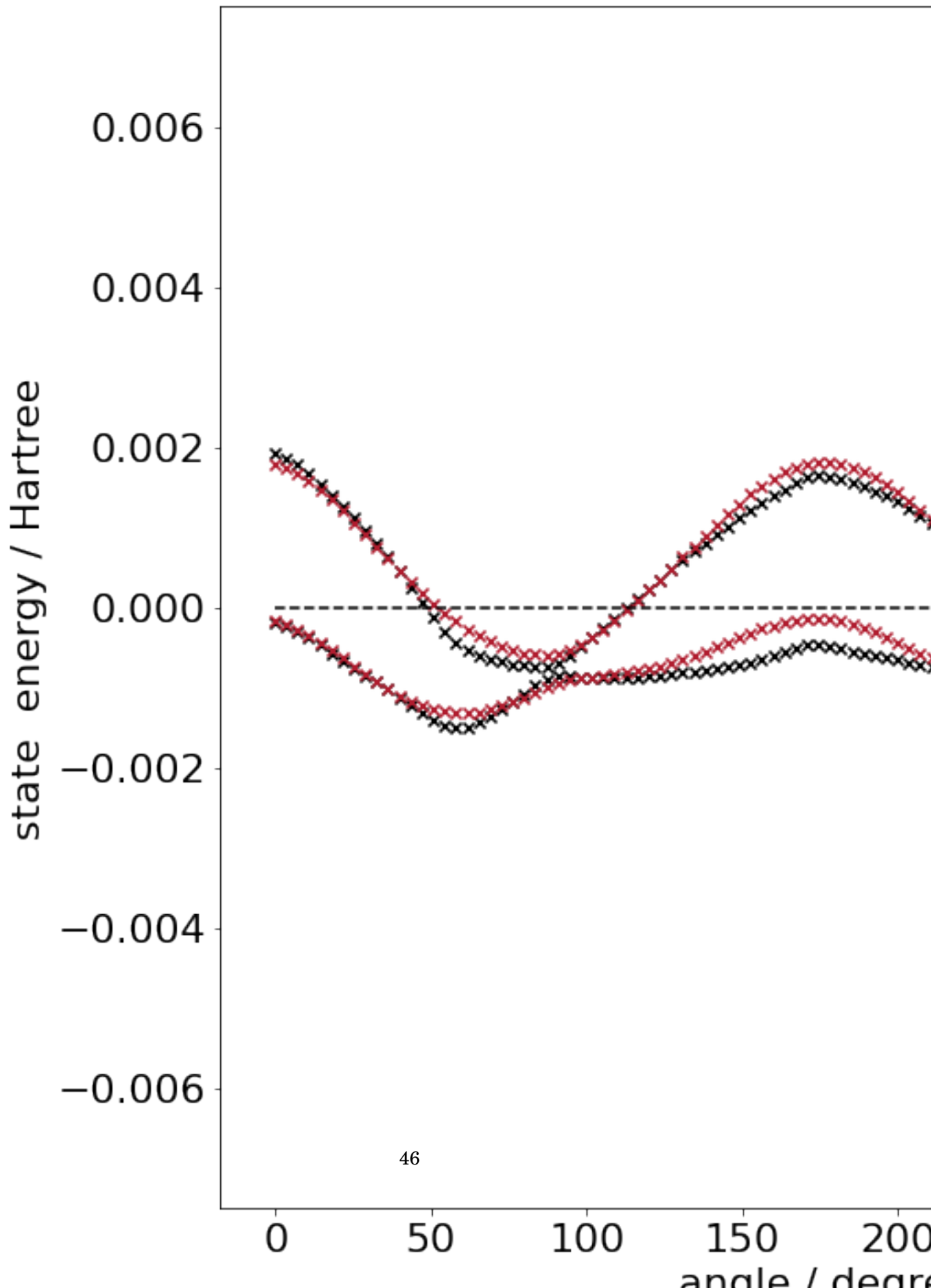


**EXCITON METHOD**

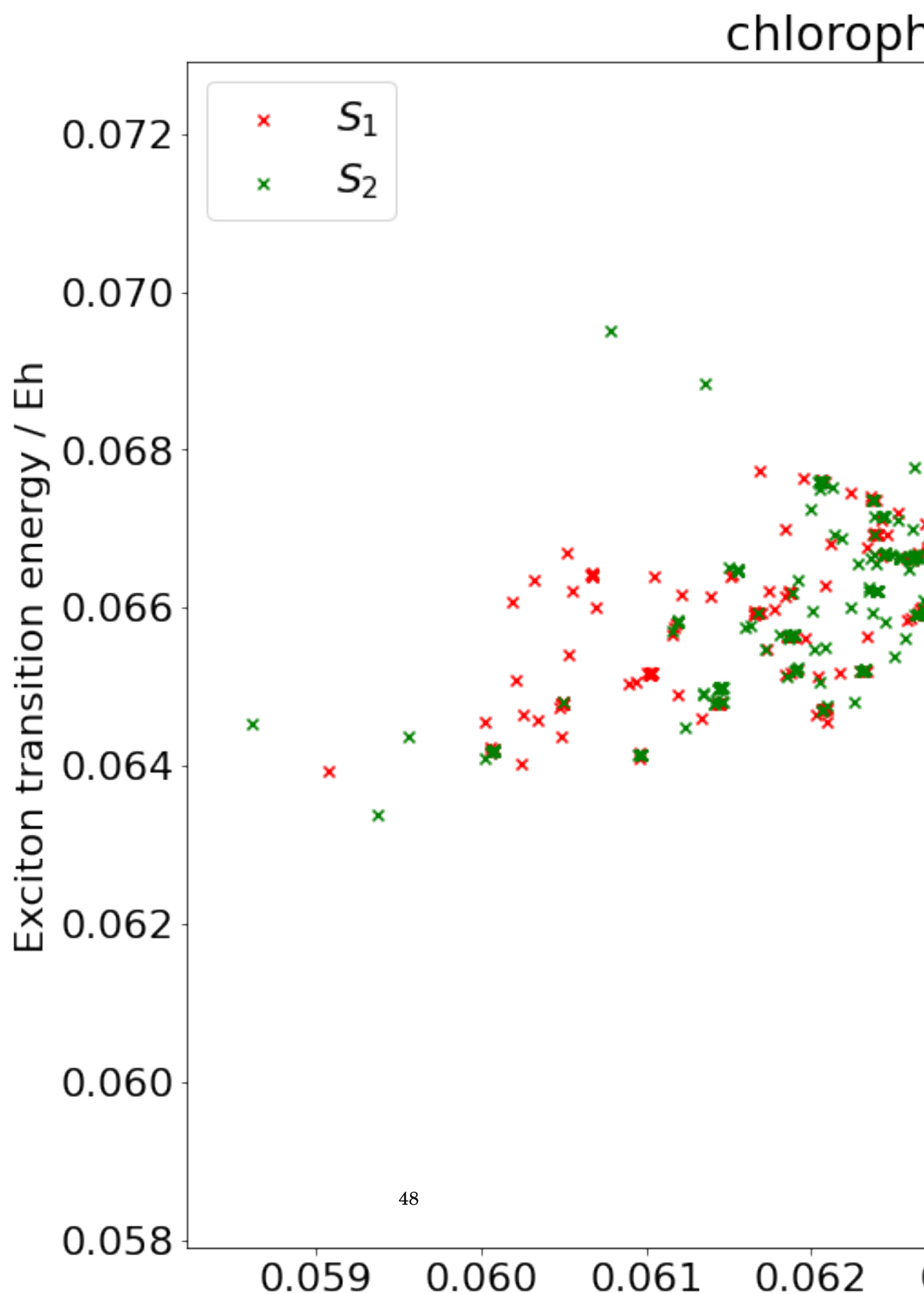
**P**reamble

**4.1 Theory****4.1.1 Exciton States****4.1.2 Embedding****4.2 Truncated Chlorophylls****4.2.1 Rotation****4.2.2 Distance****4.3 LHII Pairs****4.3.1 Assignment of States****4.3.2 Comparison**

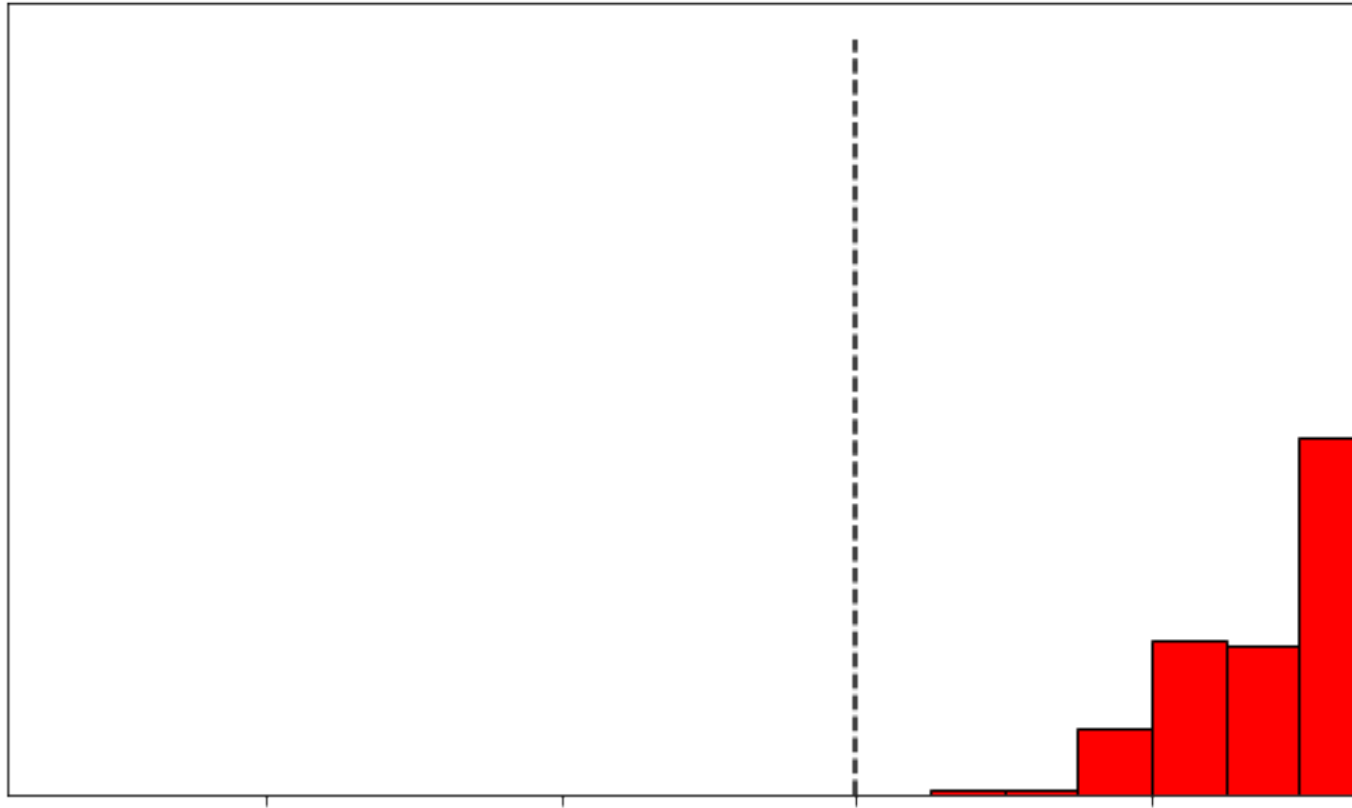
## Excited states of a ro



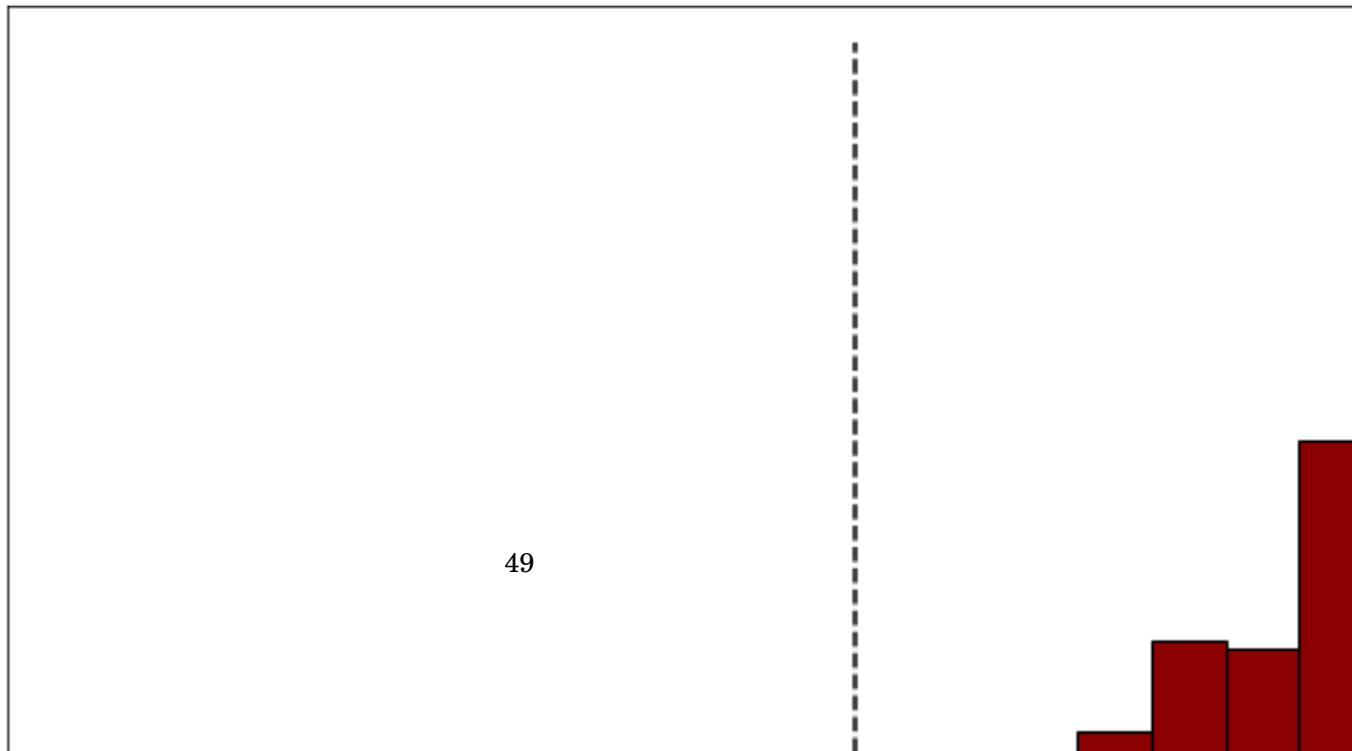




energy ordered



centre ordered

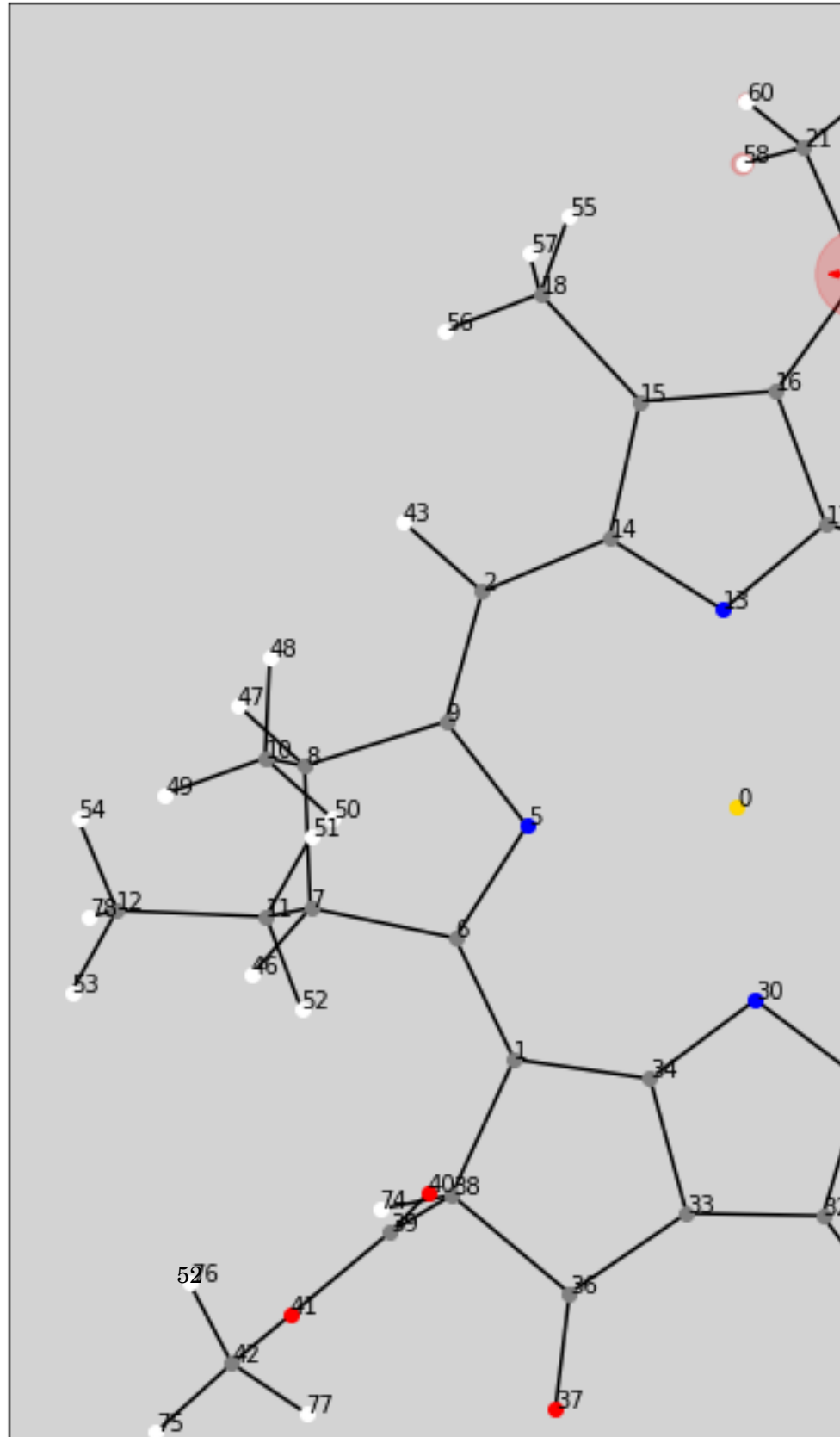


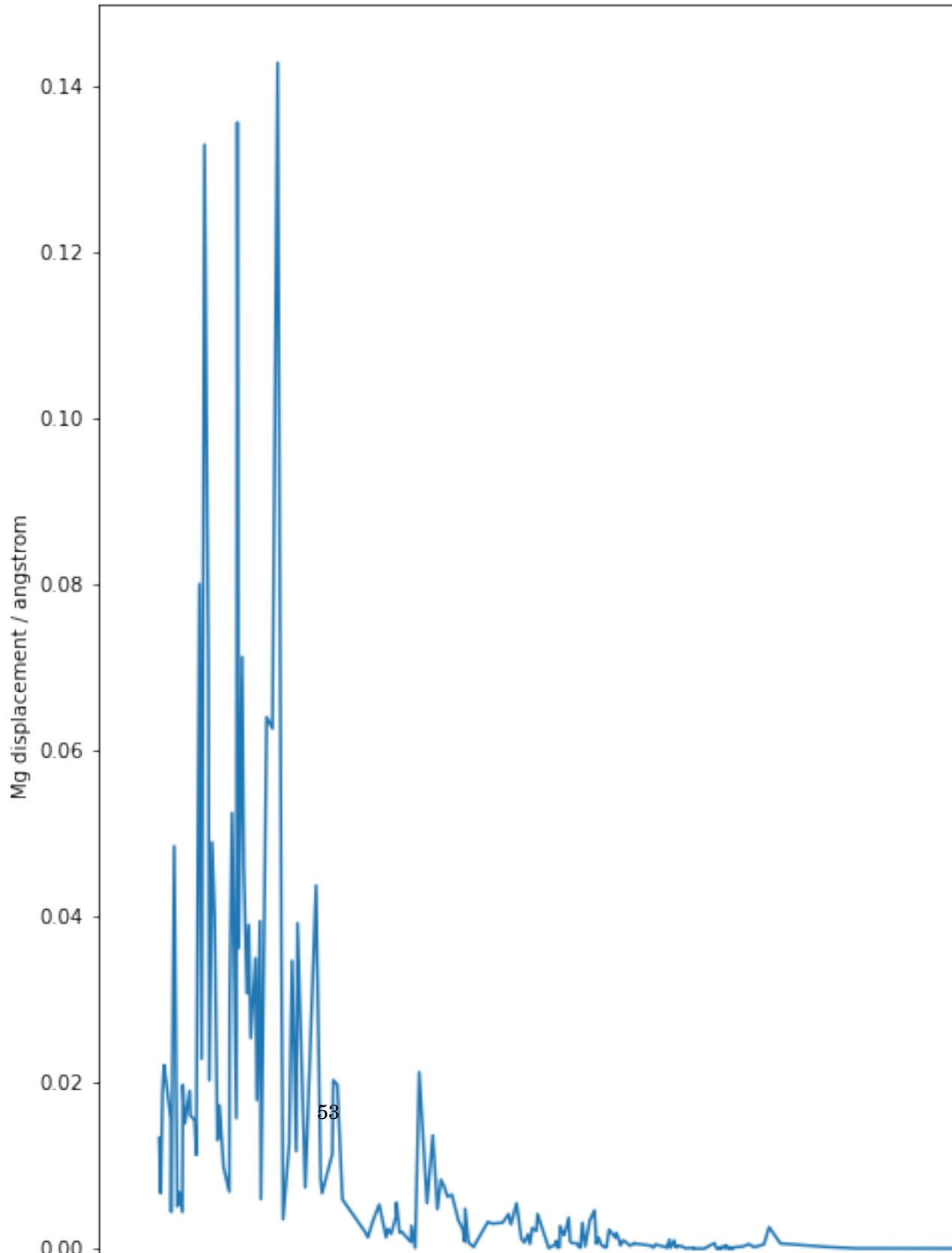


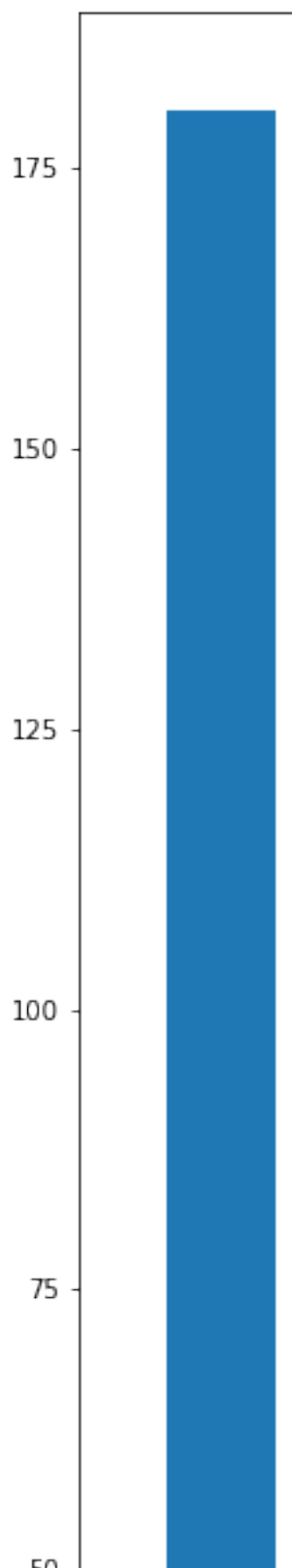
C H A P T E R

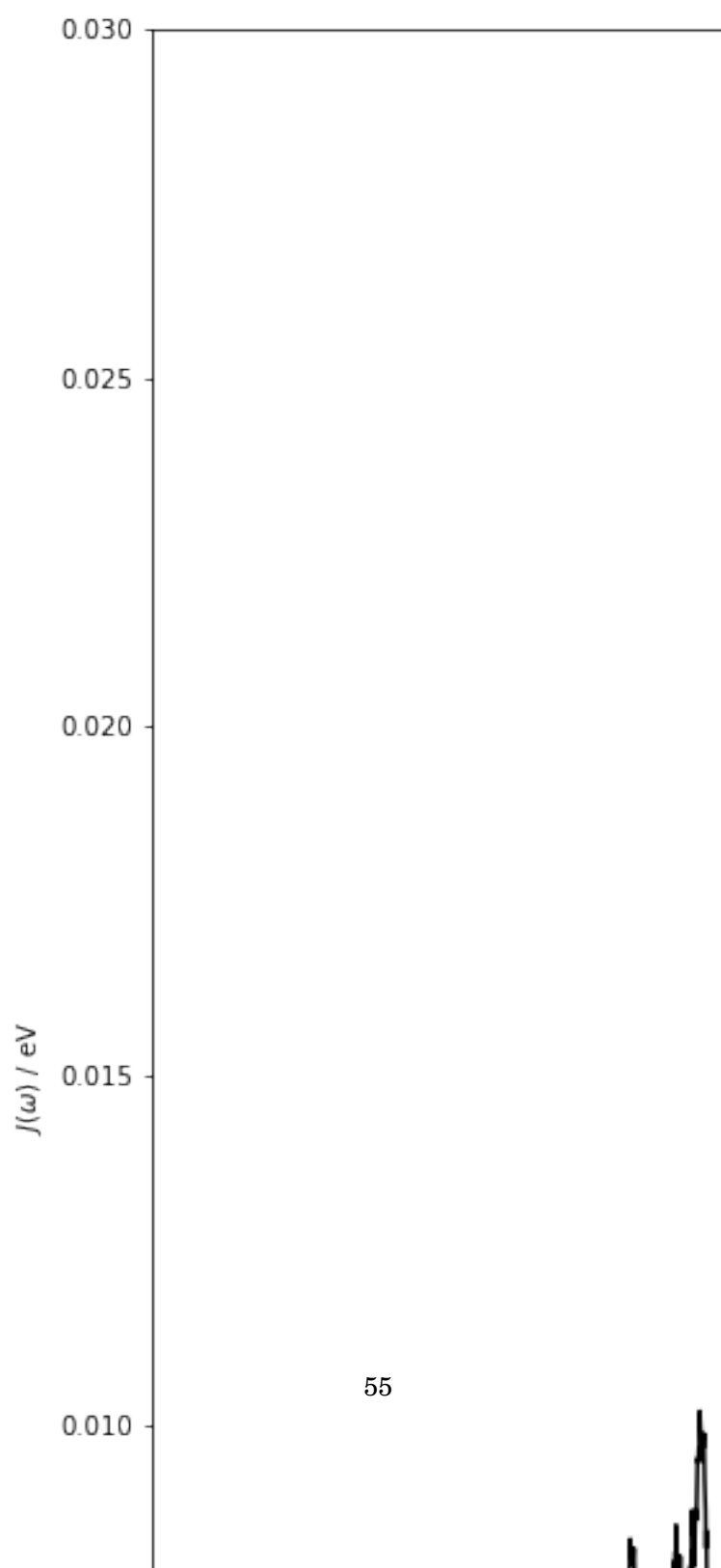


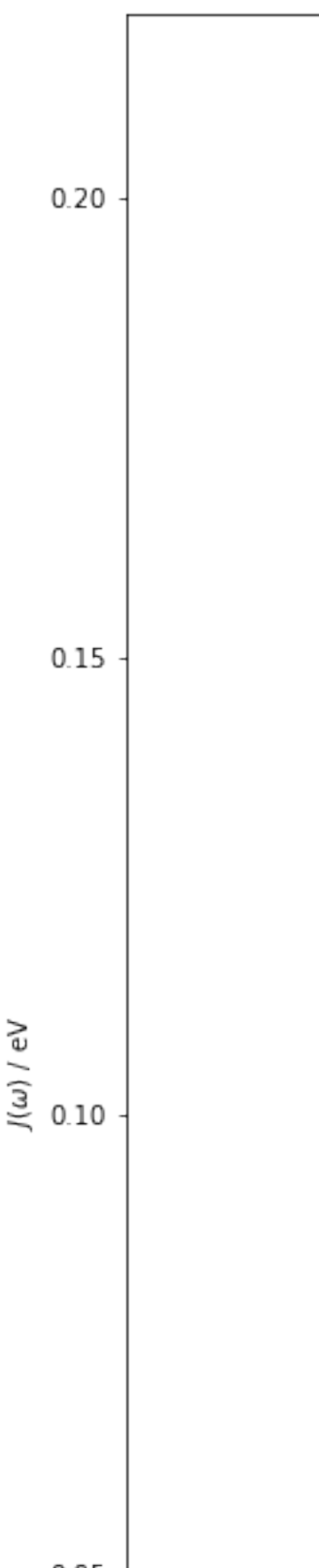
## ATOMISTIC MODELLING OF LIGHT HARVESTING COMPLEXES

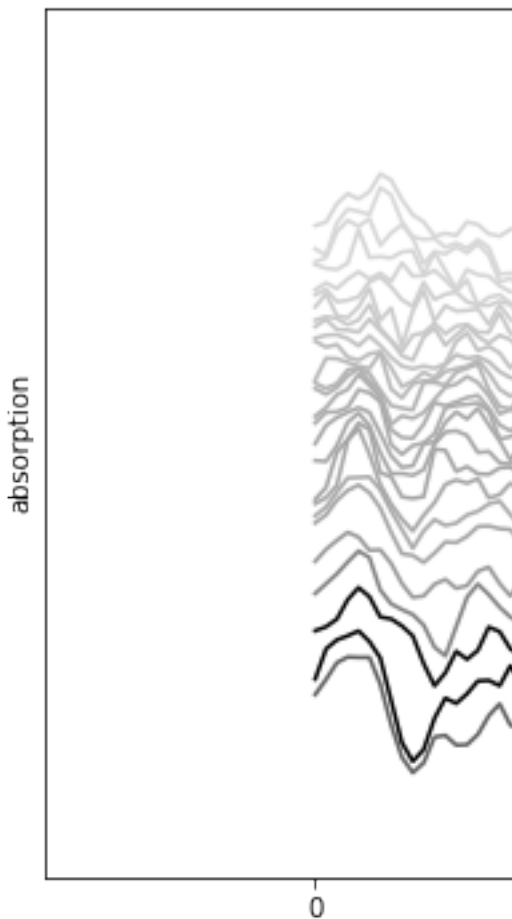


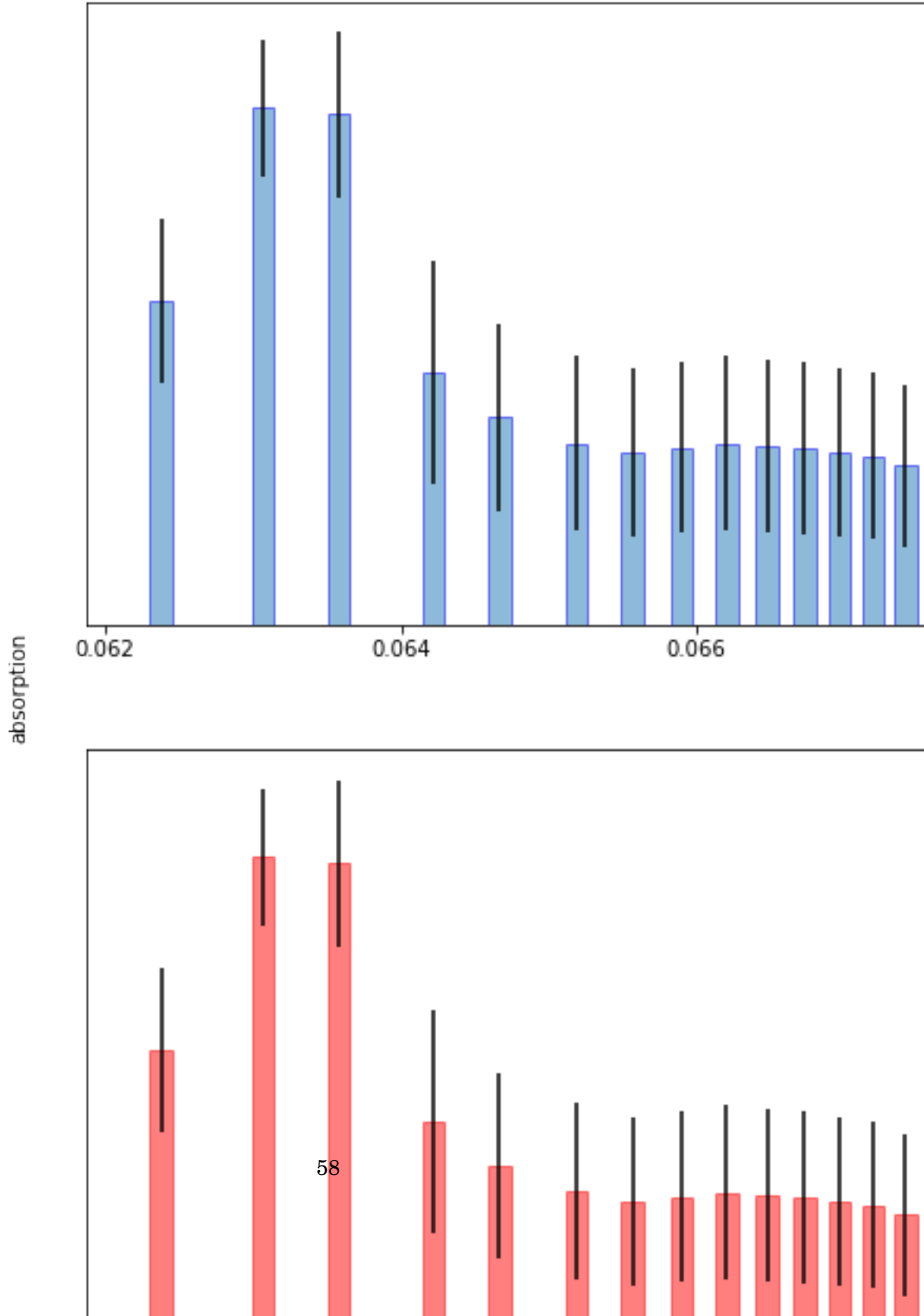












## 5.1 LHII

### 5.1.1 Spectral Density Method

### 5.1.2 Molecular Dynamics Method

## 5.2 Approximating Spectral Densities

### 5.2.1 Hessians

### 5.2.2 Huang Rhys Factors

### 5.2.3 Chlorophyll distances

## 5.3 Environmental Effects

### 5.3.1 Screening

### 5.3.2 Embedding

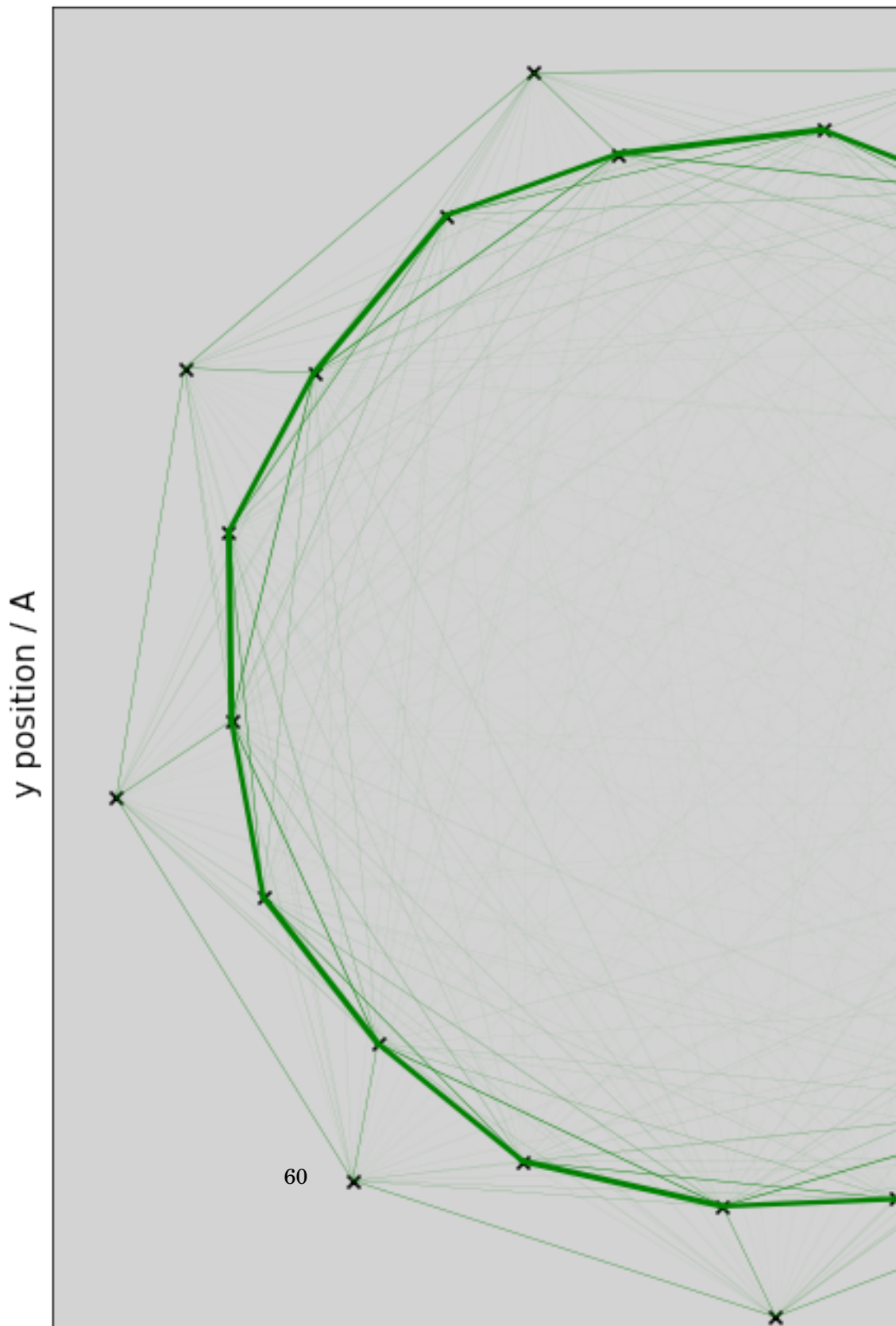
## 5.4 Sites, states and couplings

### 5.4.1 Sites

### 5.4.2 Exciton states

### 5.4.3 Coupling

## 5.5 Excitation Energies



**DISCUSSION**

Preamble

**6.1 Transition Property Approximations****6.2 Further Investigations into LHII****6.3 Coherence**





## APPENDIX A

This appendix covers the common computational details of this work. Included are the software packages, hardware used. These are not exhaustive list, and additional details are provided in the main chapters. However, wherever implementations or methodology details are missing, the information will be found here.

### A.1 Electronic Structure Codes

This project has primarily used the QCORE software that is found as part of the ENTOS project. This is a software package for DFT and DFTB electronic structure calculations that has been written as a joint venture between the Miller group in California Institute of Technology and the Manby group in the University of Bristol. It is now being hosted by Entos Inc. It is a novel C++ implementation, with a focus on modularity, functional code and modern development practices to enable easier, cleaner and more reuseable code. All novel methods discussed in the chapters have been implemented in the QCORE package.

### A.2 Computational Hardware



## BIBLIOGRAPHY

- [1] D. J. FRISCH, M. J.; TRUCKS, G. W.; SCHLEGEL, H. B.; SCUSERIA, G. E.; ROBB, M. A.; CHEESEMAN, J. R.; SCALMANI, G.; BARONE, V.; PETERSSON, G. A.; NAKATSUJI, H.; LI, X.; CARICATO, M.; MARENICH, A. V.; BLOINO, J.; JANESKO, B. G.; GOMPERTS, R.; MENNUCCI, B.; HRATCH, *Gaussian 16, Revision C.01*, 2016.
- [2] J. GASTEIGER AND M. MARSILI, *A new model for calculating atomic charges in molecules*, Tetrahedron Lett., 19 (1978), pp. 3181–3184.
- [3] A. T. B. GILBERT, N. A. BESLEY, AND P. M. W. GILL, *Self-Consistent Field Calculations of Excited States Using the Maximum Overlap Method (MOM)* †, J. Phys. Chem., 112 (2008), p. 13164.
- [4] T. GIMON, A. IPATOV, A. HESSELMANN, AND A. GÖRLING, *Qualitatively Correct Charge-Transfer Excitation Energies in HeH<sup>+</sup> by Time-Dependent Density-Functional Theory Due to Exact Exchange Kohn-Sham Eigenvalue Differences*, J. Chem. Theory Comput., 5 (2009), p. 27.
- [5] S. GRIMME, *A simplified Tamm-Dancoff density functional approach for the electronic excitation spectra of very large molecules*, J. Chem. Phys., 138 (2013), p. 244104.
- [6] S. GRIMME AND C. BANNWARTH, *Ultra-fast computation of electronic spectra for large systems by tight-binding based simplified Tamm-Dancoff approximation (sTDA-xTB)*, J. Chem. Phys., 145 (2016), p. 54103.
- [7] S. GRIMME, C. BANNWARTH, AND P. SHUSHKOV, *A Robust and Accurate Tight-Binding Quantum Chemical Method for Structures, Vibrational Frequencies, and Noncovalent Interactions of Large Molecular Systems Parametrized for All spd-Block Elements (Z = 1-86)*, J. Chem. Theory Comput., 13 (2017), pp. 1989–2009.
- [8] S. W. J. HUNT AND W. A. GODDARD, *Excited States of H<sub>2</sub>O using improved virtual orbitals*, Chem. Phys. Lett., 3 (1969), pp. 414–418.
- [9] G. KLOPMAN, V. 86, J. LINEVSKY, K. S. SESHADEVI, AND D. WHITE, *A Semiempirical Treatment of Molecular Structures. II. Molecular Terms and Application to Diatomic Molecules*, J. Am. Chem. Soc., 86 (1964), pp. 4550–4557.

## BIBLIOGRAPHY

---

- [10] P. O. LÖWDIN, *Quantum theory of many-particle systems. I. Physical interpretations by means of density matrices, natural spin-orbitals, and convergence problems in the method of configurational interaction*, Phys. Rev., 97 (1955), pp. 1474–1489.
- [11] A. V. MARENICH, S. V. JEROME, C. J. CRAMER, AND D. G. TRUHLAR, *Charge Model 5: An Extension of Hirshfeld Population Analysis for the Accurate Description of Molecular Interactions in Gaseous and Condensed Phases*, (2012).
- [12] K. NISHIMOTO AND N. MATAGA, *Electronic Structure and Spectra of Some Nitrogen Heterocycles*, Zeitshrift fur Phys. Chemie Neue Folge, 12 (1957), pp. 335–338.
- [13] K. OHNO, *Some Remarks on the Pariser-Parr-Pople Method*, Theor. chim. Acta, 2 (1964), pp. 219–227.
- [14] C. C. J. ROOTHAAN, *New Developments in Molecular Orbital Theory*, Rev. Mod. Phys., 23 (1951), p. 69.